CANCER RESEARCH CENTER (CSIC-USAL)

Pttg1 implication in cellular and physiological processes regulated by RasGrf1

DOCTORAL THESIS

Lara Manyes i Font

Salamanca, 2012

Table of contents

Abbreviations

BSA: Bovine serum albumin

bp: base pair

cAMP: 3'-5'-cyclic adenosine monophosphate

CDKs: Cyclin-dependent kinase

cDNA: Complementary DNA

DMEM: Dulbecco's Modified Eagle Medium

DMSO: Dimethyl sulfoxide

DNA: Deoxyribonucleic acid

EDTA: Ethylenediaminetetraacetic acid

EGF: Epidermal growth factor

ERK: Extracellular signal-regulated kinases

FBS: Fetal bovine serum

GAPs: GTPase activating proteins

GDP: Guanosine diphosphate

GEFs: Guanine nucleotide ex change factor

GO: Gene Ontology

GPCR: G protein coupled receptors

GTP: Guanosine triphosphate

Kb: kilo base pairs

KO: Knock out

MAPKs: Mitogen-activated protein kinases

mRNA: Messenger RNA

MTT: Dimethyl thiazolyl diphenyl tetrazolium salt

PBS: Phosphate buffered saline

PI: Phosphatidylinositol 3-kinases

PI3K: Phospholipase C

PLC: Propidium iodide

RB: Retinoblastoma

RNA: Ribonucleic acid

rpm: Revolutions per minute

RTKs: Receptor tyrosine kinase

SAPKs: Stress-activated protein kinases

SDS: Sodium dodecyl sulfate

SH3: SRC Homology 3 Domain

shRNA: Short hairpin RNA

SRE: Serum response element

TBS-T: Tris-Buffered Saline and Tween 20

TCR: T-cell receptor

WT: Wild type

Figure index

Table index

Introduction

I. RasGrf1, a guanine nucleotide exchange factor (GEF)

Both RasGrfs are multi-domain proteins that act as signaling mediators. They transmit several stimulus from receptors and second messengers to their GTPases Ras and Rac family targets [1]. RasGrf1 is able to activate a variety of small GTPases, including Ras, Rac1, M-Ras and R-Ras [2-6].
RasGrf1 is a GEF mainly expressed in the central nervous system (CNS), specially at the pyramidal cell layer of hippocampus and dentate gyrus and in the granule cell layer of the cerebellum, neocortex and some deep nuclei [7]. Its expression increases after birth at the same time that the complex neuronal network is created [8]. RasGrf1 protein has also been detected at lung and pancreatic tissues [9].

1. Signaling mediated by RasGrfs

a. Activation of RasGrfs responding to a intracellular calcium rise

A rise in the intracellular calcium levels induces activation of both RasGrfs which, at the same time, activate Ras [10]. This process is initiated with binding of calcium-activated calmodulin to the IQ domain on RasGrf1 [11], in a process that involves the amino terminal PH1 and CC domains, facilitating RasGrf1 protein subcellular localization [12]. It has been also seen than DHPH2 domains are necessary for a correct activation of ERK upon induction of these cells with ionomycin [13]. RasGrf1 activation by ionomycin is mediated by Cdc42 and it is normally done in plasmatic membrane [14].

Stimulation of NMDA receptor (Fig. 1 A) induces opening of calcium channels nad the increase of intrecellular calcium levels in neurons. Interaction between RasGrf1 and the NR2B subunit of the NMDA receptor helps coupling these Ca^{+2} increases with activation of Ras signaling cascade. In a study using primary neurons, it has been that a dominant negative of NR2B blocks activation of ERK stimulating receptors with NMDA and bicuculline [15]. Seemingly, another study using hippocampus mouse slices and cultured neu-

rons, describes that activation of NMDA receptors leads to phosphorylation of RasGrf1 in serine 916 and ERK activation, in a process that requires the action of calmodulin kinase kinase and calmodulin kinase I [16]. In contrast, two later works using RasGrf1 and RasGrf2 KO mice show that RasGrf1 activation by NMDA receptor contribute more to activation of p38MAPK than to ERK activation and suggest a relationship between this activation and LTD (long term depression); meanwhile, LTP (long term potentiation) would be mediated by interaction among NR2A and RasGrf2 that would activate ERK signaling pathway [17, 18]. However, in cortex sections of transgenic NR2B mice, it has been described an improvement of LTP when downregulating RasGrf1 expression [19], which can indicate a different function for this GEF depending on the cerebral area.

In summary, respective interactions of RasGrf family members with different NMDA receptor subunits seem to be responsible of a first level of specificity engaging those GEF to calcium channels. The second level could be regulated by diverse scaffold proteins which determine RasGrf interactions with specific effectors [20, 21].

Receptor of AMPA activation of RasGrf1 and RasGrf2 in cortical slices of post-adolescent mice is calcium dependent [22]. When induced by its agonist, serotonin receptor coupled to heterotrimeric G protein, appear to need the interaction between calcium/calmodulin and RasGrf1 as well as RasGrf1 phosphorylation by PKA in vitro to induce ERK phosphorylation, [23].

Calcium mediated signaling in pancreatic β cells is regulated by Grf β. This shorter transcript for RasGrf1 locus acts as a negative dominant modulator, probably preventing the interaction of RasGrf1 to upstream activators or by disrupting its intracellular localization. In CHO cells it has been described that calcium activation of m-calpain proteases leads to the downregulation of RasGrf1 expression and its phosphorylation in S731 by p35/CDK5, raises its sensibility to calpain degradation. This process leads to into nuclear condensation and disorganization [24].

b. RasGrfs1 activation G protein coupled receptors (GPCR)

Extracellular stimuli that specifically interact with transmembrane receptors coupled to heterometrimeric GPCR are able to activate several second messengers and channels to initiate a great variety of intracellular signaling pathways. Receptor stimulation by its specific ligands induces splitting of heterotrimeric G protein into their subunits Gα-GTP and Gβγ, which there are free to interact specifically with other components downstream in the intracellular pathways [25, 26]. Gβγ dimers with PH domains of proteins like PLCγ, spectrine or IRS [27]. Serum stimulation of NIH3T3 cells induces RasGrf1 GEF activity, followed by its hyperphosphorylation. In this work is suggested that GPCRs, but not RTKs, are responsible for RasGrfs activation, since this is suppressed when cells were pre-trea-

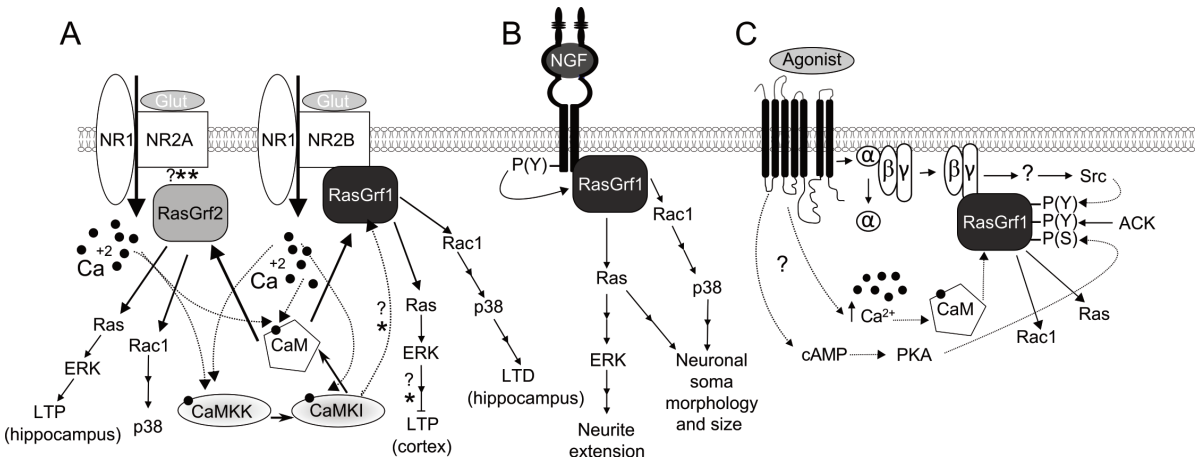

Fig 1. Main pathways of RasGrfs activation. **A.** NMDA receptor induced Ca^{+2} signaling integration mediated by RasGrf. RasGrf1 binds to the NR2B subunit of the NMDA receptor and based on indirect evidences, a similar interaction has been hypothesized for RasGrf2 and NR2A (?**). Calmodulin kinase I (CaMKI) (?*) is suggested to directly bind RasGrf1. RasGrf1 intracellular signaling activates LTD response and it is proposed to also inhibit LTP response. **B.** Receptor tyrosin kinase (RTK) TrkA phosphorylates and activates RasGrf1. **C.** G-protein-coupled receptor (GPCR) activates RasGrf1. Phosphorylation of serine and tyrosin residues is needed for RasGrf1 activation. P(Y), phosphotyrosin. P(S), phosphoserine. Modified from [1].

ted with pertussis toxin (PT) but not with genistein [28]. In CHO cells it has been described the same sensibility to pre-treatment with PT when inducing with LPA or serum, but not with PDGF [29]. The over-expression in vitro of the human muscarinic receptor and stimulation with carbacol causes the phosphorylation of RasGrf and induces its GEF activity [30].

RasGrf1 phosphorylation induced by stimulation with LPA involves its serine residues. Calcium depletion inhibits this activation suggesting a model in which RasGrf1 would act like a signal integrator [31]. RasGrf1 phosphorylation in S916 is achieved upon induction of PC12, COS-7, forebrain sections and rat cortex with NGF, as well as with carbacole or forskoline, when stimulating endogen Trk receptors. In this same work, the differentiation of PC12 cells analysis directly correlates with S916 phosphorylation, H-Ras expression and neurites growth [32]. The same serine is phosphorylated in HEK293 cells when overexpressing GPRC 5-HT4 receptors and after stimulation with serotonin [23, 33].

Activation of GPRCs has been also associated to RasGrfs ability to activate Rho family members. In spite that the description of RasGrf1 DHPH domains was an early event, studies failed to find a GEF activity towards Rho family members. The first study to show that RasGrf1 can activate Rac1 had to overexpress G protein βγ subunits in 293T cells [34]. In a later study, stimulation with LPA has been shown to induce Rac1 activation by RasGrf1 leading to JNK and c-fos promoter activation [5].

c. RasGrfs activation by RTKs and non-receptor tyrosine kinases

RasGrf1 N-terminal region interacts with the HIKE domain of TrkA which tyrosine phosphorylates its PH1 domain, in a process where ectopic transfection of RasGrf1 increases NGF capacity of promoting cell differentiation when inducing neurites growth in PC12 cells [35]. This neurites extension process requires activation from H-Ras and ERK but it is independent of Rac1 and PI3K pathways. In what seems to be an unrelated process, RasGrf1 coordinates Rac1 and H-Ras pathways in a PI3K/AKT independent manner to induce soma extension in PC12 cells, what could be related to LTP generation in a more physiological environment [36]. Recently, it has been described that this neurite extension process I H-Ras and Rac1 dependent [37].

Non-receptor tyrosin kinase Src mediates GPCR signaling, phosphorylates RasGfr1 in vivo and activates its Rac1 GEF function [38]; another work by Giglione et al. found that Src has no kinase activity over RasGfr1, in this study Src also seems to keep Ras signaling activation by phosphorylating p120GAP, inhibiting its GAP activity [39]. The difference between these articles is that in the first one, they used the 293T cell line and in the second the analysis was performed in vitro, suggesting that other components are required for activation of RasGrf1 by Src. On the study by Giglione et al., Lck, another tyrosine kinase from the Src family, is also able to phosphorylate and upregulate RasGfr1 GEF function [39]. ACK1, a non-receptor tyrosine kinase activated by Cdc42, also phosphorylates and activates RasGrf1, which suggest a possible relationship between this kinase and Ras signaling pathway [40]. Cdc42 modulates RasGrf1 [41, 42] and RasGrf2 [43] activity. Finally, RasGrf2, the same as RasGrf1, is activated when inducing T cells receptor in a process that seems to require the tyrosine kinase activity of a Src family member [44].

2. RasGrf cellular functions

a. Cell proliferation

RasGrf1 gene was first identified because of its capacity to restore the growth phenotype in yeast lacking the CDC25 locus [45]. In mouse fibroblasts, its over-expression induces cellular transformation and increases proliferation [46, 47], the same as in NIH3T3 cells when transfected with constructions constitutively located at the membrane [48]. The integrity of RasGrf1 domains implicated in both Ras and Rac1 activation appears to be necessary to induce proliferation, showing essential collaboration between pathways [41]. It is important to highlight that physiologically RasGrf1 is only expressed after birth and mainly in the Central Nervous System (CNS), where cellular proliferation is low.

RasGrf2 has been related to the control of proliferation in immunological context, where it has been seen that this GEF participates in T cell receptor signaling [44].

b. Differentiation

It has been shown that RasGrf1 promotes neuronal differentiation in studies where neurites elongation is measured in SK-N-BE or PC12 cell lines. This is achieved in presence of neurotropic stimulus as retinoic acid and NFG respectively, but also co-expressing RasGrf1 and H-Ras, in a process Rac1- and PI3K- independent [32, 35, 36, 49].

In another work, it has been shown that SCLIP protein, microtubules destabilizing, is capable of inhibiting neurites formation induced by RasGrf1 in PC12 cells mediated by Rac1 activation but not H- Ras [50]. As RasGrf1 is capable to interact with microtubules [51], there is a hypothesis that holds that this inhibiting effect is mainly due to a possible RasGrf1 function in the cytoskeleton, but nit due to its intrinsic GEF activity [50].

c. Cellular organization and morphology

An increase in soma size of ≈25% is observed in a population of PC12 cells cotransfected with RasGrf1 and H-Ras. This phenotype seems to be independent of GTP binding to Ras but dependent on Rac1, PI3K and Akt contribution [36].

In a study using COS-7 cells and cultures of rat cortical neurons, has been observed the RasGrf1 implication in nuclear organization control. p35/Cdk5 phosphorylates RasGrf1 and provokes its degradation by m-calpain, in order to regulate the RasGrf1 expression levels and Ras/Akt pathway activation [24]. In the same type of neurons they describe that RasGrf2 phosphorylation by p35/Cdk5 provokes an accumulation of MaP1b, associated to cytoskeleton [52].

d. Excitability and neuronal responses

Excitability and synaptic plasticity are neuronal processes related to RasGrf1 activity due to its subcellular localization in synaptic junctions [53] and hyperexcitability has been seen for RasGfr1 deficient neurons, probably caused by changes in the ionic balance of the plasma membrane [54]. Both RasGrfs have a role in neuroprotection. In episodes of experimental ischemia the absence of both GEFs greatly increased cell apoptosis [55]. This result was confirmed in a study using haloperidol treatment, which leads to RasGrf1 dissociation of the NMDA receptors, activation of JNK and an increase of apoptosis [56]. Another study has also shown that in crystalline epithelial rabbit cells, activation of the Ras/ERK pathway by RasGrf2 rises levels of intracellular p53 and caspase 3 activation, which points to its implication apoptosis, at least in this cell type [57].

e. Carcinogenesis

RasGrf1 might be related to cellular invasion and metastasis because of its ability to control the expression of several matrix metaloproteins (MMP), as observed in human melanoma cell line [58], as well as in fibroblastic synoviocytes of rheumatoid arthritis patients [59]. In another recent work authors propose that elimination of differentially methylated regions in RasGrf1 locus of very small embryonic/epiblastic stem cells (VSELs), would lead to tumor formation [60].

Although RasGrf2 role in tumorigenesis has not been clearly defined, several studies have described the existence of reduced levels of this protein in diverse human and mice tumors, which is usually associated to an aberrant methylation of its genomic locus [61-64]. Furthermore, genetic deficiency in RasGrf2 locus plus alterations in the Vav1 locus could be related to lymphomagenesis and metastatic processes [65]. Calvo et al. have recently discovered that RasGRF2 acts as tumor suppressor by blocking rounded movement. The process requires inhibition of the Cdc42 activation independently of its capacity to activate Ras, although they describe both RasGrfs as modulators of Cdc42 activity [66].

3. RasGrf1 and RasGrf2 animal models

RasGrf1 high and almost exclusive expression at the CNS predicted an important role for this GEF in neurological processes. This have been confirmed when phenotype of KO mice was analyzed. The first work describing the KO mice for this loci showed that mice display impaired amygdala dependent learning as a result of LTP errors, but hippocampal learning was not affected [67]. Another work using a different KO mice line described that their animals had deficiencies in generating LTD, which would produce defects in hippocampus dependent learning [17, 68]. These contradictory results are probably due to different strategies in gen deleting expression and/or because of the different KO mice background lines.

RasGrf1 KO mice have defects in photoreception, suggesting a role in the retina. Electroretinographic analysis has shown that the mutant mice have strong defects in light perception, a phenotype which aggravates with age [69]. Recently, a “GWAS” study identified RasGrf1 as susceptibility locus associated to myopia and refractive problems in humans, which agrees with crystalline alterations observed in those animals [70].

These KO mice have reduced tolerance to chronic administration of delta-9-hidrocannabinol (THC). It seems that RasGfr1 is responsible for the adaptation of the cannabinoid receptor CB1 to the drug in cerebellum and striatum [71, 72] and its elimination removes changes in cerebellar synaptic plasticity after chronic treatment with THC [73]. In response to cocaine treatment RasGrf1 KO mice show less locomotor sensibility and conditioned place preference (CPP) [74].

RasGrf1 KO mice display a 15-25% reduction in body size, which manifest its importance in post-natal growth [68, 75, 76]. In phenotypical characterization of these mice, authors found lower levels of growth hormone factor hormone pituitary of KO mice, suggesting that RasGrf1 signaling is very important in hypothalamus and a defect in growth hormone release as a possible cause of the problem [76, 77].

Analysis on a different strain of KO mice also revealed that they have glucose intolerance, reduced insulin plasma levels and diminished pancreatic β-cell mass, supporting the idea of an important role of RasGrf1 in β-cell proliferation control and neogenesis [78].

The analysis of RasGrf2 deficient mice found no gross significant differences [75] and only subtle phenotypic changes have been found when molecular signaling in their brain was studied, discovering a reduced ERK activation when inducing with NMDA [17]. Elimination of this gen in combination with RasGrf1 produces an increase in neuronal damage induced by ischemia compared to simple KO or wild type mice, suggesting an overlapping, protective role for both RasGfrs in stroke-induced neurotoxicity, probably through a reduction of CREB phosphorylation and activity [55]. It has also been shown a role for this GEF when crossing KO mice with mice KO for Vav1, a guanine nucleotide exchange factor of Rho family GTPases. Analyses of deficient RasGrf2/Vav1 mice have demonstrated that RasGrf2 is an additional component of the signaling machinery involved in T-cell receptor and NF-AT-mediated immune responses. Furthermore, the RasGrf2 and Vav deficiency also exerts a synergistic effect on lymphomagenesis and metastasis in these KO animals [44, 65].

It is important to notice that there is a high similitude between some phenotypes observed in KO mice for RasGrf1 and animals deficient for other molecules. For example Pttg1 [79], S6K1 [80, 81] or Cdk4 [82], whose phenotypes match with RasGrf1 reduction in body size and diminished pancreatic β-cells mass, suggesting a role in the same signaling pathways [1]. Our laboratory has obtained evidences of a possible role for RasGrf1 in the regulation of Pttg1 expression. Using microarray analysis, Pttg1 expression seems to be affected in the retina [69], in Langerhans islets, hippocampus, olfactory bulb and cortex of KO RasGrf1 mice there is a significant reduction of Pttg1 expression (data not published).

II. Pituitary tumor transforming gene (Pttg1)

Pttg1 was isolated in 1997 from rat pituitary tumor cells [83]. *PTTG1* encodes a multifunctional protein involved in cell cycle regulation, DNA damage and reparation, direct transcriptional activity, organ development and metabolism. Pttg1 is an oncogene related to neoplastic transformation. It was identified, because of its structural homology, as the vertebrate securin, a critical yeast protein involved in the regulation of sister chromatids separation [84].

In non-malignant tissues, PTTG1 is highly expressed in testis and thymus, and lower levels are also present in the placenta, colon, small intestines, brain and pancreas [85-87]. Increased levels of PTTG1 were found in thyroid [88], pituitary [89-92], colorectal [93], esophageal [94], liver [95] and lung carcinomas [96], in breast, ovarian and testicular tumors [97] and in uterus leiomyoma [98].

1. Physiological function

a. Securin/replication

In metaphase, cohesin complex maintains sister chromatids together, an essential process for the correct bipolar orientation of chromosomes in the mitotic spindles [99]. Securin binds separase to inhibit its proteolysis activity [100-103]. In vertebrates, cyclinB-Cdk1 also acts in this process by inhibiting phosphorylation of separase [104, 105]. During metaphase-anaphase transition, when sister chromatids are aligned, cyclinB/Cdk1 phosphorylate the APC complex that ubiquitinates securing protein. This process leads to securin degradation by the proteasoma, meanwhile cyclinB is also degradated. The release of separase provokes cohesion complex degradation, allowing sister chromatid separation and segregation [106]. Pttg1 interacts with Sp1 to exert this modulation of the spindle-assembly checkpoint in a p21-independent process [107].

b. DNA damage repair

In mammalian cells, PTTG1 binds Ku-70, the regulatory subunit of DNA-PK, an enzyme involved in double helix DNA damage repair. This association is lost in response to DNA damage, suggesting a role for PTTG1 in mitosis blockade while reparation is on course [108].

c. Transactivation activity

Dominguez et al. discovered the Pttg1 function in transactivation [85] when they realized that Pttg1 carboxi terminal domain was similar to other transcription activators described in eukaryotes [109]. Deletion and mutagenesis studies suggest that 3D Pttg1 structure is

important for this function and permitted to distinguish critical transactivating sites [110]. It has been described a MAPK consensus phosphorylation site in Pttg1 transactivation domain [110] and Pttg1 interaction with MEK1 is necessary to mediate MAPKs transactivation function [111].

PTTG1 regulates pituitary hormone expression. Overexpression of its carboxi terminal fragment in lactosomatotropic GH3 cells diminished in 10 folds prolactin mRNA expression and its secretion. In contrast, GH (growth hormone) mRNA is increased over 4-folds [112].

In a ChIP-on-chip study, 700 promoters were found enriched upon immunoprecipitation of PTTG1. 400 of them were classified in three functional groups: cell cycle, metabolic control and signal transduction pathways. These promoter regions where specially enriched in Sp1 transcription factor [107]. In another work, the expression of five genes was found to be upregulated when inducing Pttg1: c-myc, PKC β-1, MEK1, MEK3 and HSP70. In this analysis, Pttg1 residues 60-118 were identified as essential for DNA binding and for its transcriptional function [113].

2. Tumorigenic functions

a. Cell proliferation

Controversial data has been published regarding the role of Pttg1 in proliferation. In some studies Pttg1 overexpression increases cell growing [87, 113, 114] but in others reduces it [83, 115] and even produces a cell cycle blockade, provoking accumulation of the cells in the G2/M phase [116-118]. In contrast, downregulation using siRNA (short interference) point to a cell line-independent inhibition of proliferation [95, 119, 120].

In NT-2 cells it has been shown that low levels of PTTG1 expression promote proliferation and high ones reduces it or even block cell cycle [121]. The state of PTTG1 phosphorylation also affects this process. The presence of phosphorylated PTTG1 reduces proliferation, while without this phosphorylation growth rate increases in NIH3T3 transfected cells [122].

b. Cellular transformation and aneuploidy

PTTG1 transforming ability is well known *in vitro* and *in vivo* [83, 86, 87, 113, 114, 123]. In H1299 lung cancer cells, PTTG1 accumulation inhibits mitosis progression and chromosomes segregation without affecting directly cytokinesis, leading to the induction of chromosomal instability and aneuploidy [124]. In HCT116 human colorectal cancer cells, PTTG1 inactivation by homologous recombination provokes chromosomal loss, aberrant

anaphases and impaired chromosomal segregation [125]. Another study using these cells showed that chromosomal loss was transient and, after few passes, cells were able to maintain a stable karyotype. They concluded that compensatory mechanisms should exist in human cells for chromosomal segregation [126].

c. Apoptosis

PTTG1 expression levels influences also apoptosis. It has been suggested a Pttg1 involvement in proapoptotic processes, like induction of p53 promoter [117], but also in apoptotic blockade by binding p53 protein [118]. These results suggest a PTTG1-mediated tumorigenic mechanism, because the inhibition of p53-dependent apoptosis by overexpression of PTTG1 would explain why tumorigenic cells survival in the presence of functional intracellular p53 [118, 127].

d. Angiogenesis

In colon cancer a strong correlation has been found between PTTG1 and tumor vascularization, an important process for tumor development. In pituitary, estrogen-stimulated PTTG1 expression and angiogenesis match with FGF-2 and VEGF-A (vascular endothelial growth factor) pituitary induction [128]. PTTG1 bounds to PBF (Pttg1 binding protein) induces FGF-2 expression by directly activating its promoter [129] but the mechanisms of VEGF induction are unknown.

6. Pttg1-/- murine model

Pttg1 KO mice are viable and fertile, although females are subfertile compared to WT and heterozygote mice. They show testicular and splenic hypoplasia, thymus hyperplasia and thrombocytopenia, with normal megakaryocytes in the bone narrow [130]. They also show a diminished body weight [131]. Pttg1 KO fibroblasts show delayed progression of the G2-M transition and aberrant chromatid separation [125, 130]

Pttg1 KO mice show impaired glucose homeostasis that leads to develop diabetes in mature males. Its development is related to no autoimmune cellular damage, insulinopenia and a reduced β cell mass [79]. Before diabetes symptoms show up, β cell mass reduction and diminished proliferation was already evident in the islets. β cell pleiotropic nucleus suggest defects in cellular division [79]. Postnatal apoptosis and senescence in adult mice was described for these cells, probably because DNA damage accumulation [132]. Pttg1 KO male mice phenotype was rescued by gonadectomy and estradiol administration, although no morphological changes were found in β cells. Hormonal therapy using sexual steroids were able to prevent late diabetes by increasing insulin sensibility, probably by augmenting serum adiponectin [133].

Data and phenotypes obtained in the described studies point to function similarities between proteins in the organs which analysis we decided to execute: hippocampus in the brain and Langerhans islets in the pancreas. In this thesis we have focused into mice spatial memory and glucose homeostasis.

Hypothesis and aims

Hypothesis

In a previous work from our lab by comparing the transcriptional profiles of WT and RasGrf1 KO mice retina we found that the Pttg1 was among those genes whose expression was more strongly affected [69]. In a similar analysis of mouse pancreatic islets we found that Pttg1 was seriously affected upon RasGrf1 elimination (unpublished data).

Our main hypothesis for the present study is that Pttg1 expression is dependent directly or indirectly on RasGrf1 signaling. Secondary hypothesis consists in that common phenotypes observed in simple RasGrf1 and Pttg1 KO mice would have the same molecular bases, altering the same signaling pathways.

Aims

1. To analyze whether Pttg1 expression is controlled by RasGrf1.
2. To study in vivo if RasGrf1 and Pttg1 have separate or overlapping functions, the next specific aims are proposed:

1.1 Generation and characterization of PC12 cell line clones with stable silencing of RasGrf1 and Pttg1 using short hairpin RNA.
1.2 Characterization of RasGrf1 intracellular pathways in the above mentioned clones.
1.3 Analysis of Pttg1 promoter activity upon the use of several cellular stimuli.

2.1 Study of RasGrf1 KO, Pttg1 KO and RasGrf1-Pttg1 KO mice spatial behavior.
2.2 Study of glucose tolerance test in the RasGrf1 KO, Pttg1 KO and RasGrf1-Pttg1 KO mice.

Materials and methods

I. First chapter of results

1. Bioinformatics tools

In the research of Pttg1 transcription factors we used the 2.3 kb sequence at 5' from ATG start codon for Pttg1 transcription. TFSEARCH ver 1.3 ©1995 Yutaka Akiyama (Kyoto University) searches for high correlated fragments within the introduced sequence in the program data base TFMATRIX (www.bioruby.org). It contains the profiles for transcription factors binding sites profiles (E. Wingender, R. Knueppel, P. Dietze, H. Karas (GBF-Braunschweig)).

Exploration and analysis of interactome networks at systems level requires a unification of the biomolecular elements and annotations that come from many different high-throughput or small-scale proteomic experiments. Only such integration can provide a non-redundant and consistent identification of proteins and interactions. APID2NET [134] is an open access tool, included in Cytoscape [135], an open source software platform available online, that allows surfing unified interactome data by quering APID server and facilitates dynamic analysis of the protein-protein interaction (PPI) networks. The program is designed to visualize, dynamically explore and analyze the proteins and interactions retrieved, including all the annotations and attributes associated to such PPIs.

2. Cellular culture

PC12, COS1 and 293T cells were grown in DMEM media complemented with glutamine 2mM, penicillin 50 units/ml and streptomycin 50 µg/ml (all from Gibco, Invitrogen). COS1 and 293T cell lines were also supplied with fetal bovine serum (FBS) 10% and PC12 cells, with FBS 5% and horse serum (HS) 10% (both from Gibco). BTC3 cells were grown in RPMI media complemented as COS1 and 293T media. Cells cultures were maintained in polystyrene plates (BD bioscience) and in 5% CO2 at 37°C. For COS1, 293T and BTC3 cells were split into new plates using TrypLETM (Gibco).

All experiments were performed with subconfluent cultures. For signaling studies, cells were starved during 4h, with completed media without serum. For stimulation the compounds were added to the starvation media at the indicated concentrations.

.- Nerve Growth Factor(NGF) 100 ng/ml (Promega)
.- Ionomycin 100 nM (Sigma)
.- Epidermal Growth Factor (EGF) 60 ng/ml (Peprotech)

3. shRNA lentiviral transdution for the generation of stable silenced clones

To produce RasGrf1 and Pttg1 deficient PC12 cell line we infected them with lentiviral MISSION® shRNA particles (Sigma). RasGrf1 (NM_011245), Pttg1 (NM_013917) or a non-target construction (SHC002V) as control was used following the manufacturer's protocol. We generated RasGrf1 or Pttg1 stable silenced individual clones.

Pttg1 expression analysis was done in G2/M synchronized cells by adding 500 ng/ml nocodazole (Sigma) for 12h.

4. MTT proliferation assay

This technique evaluates cellular proliferation by using tetrazolium salt, 3-4,5 dimethylthiazol-2,5 diphenyltetrazolium bromide (MTT), that it is reduced to formazan in viable and metabolic active cells. In this process the compound turns hydrophobic and purple, so it is possible to solubilize it with isopropanol and measure the color. Each day, a plate containing the cells for a particular time point, was incubated during 2 hours in media supplied with MTT 10%. Optical density measurements were carried out using a scanning spectrophotometer Ultra Evolution Microplate Reader (TECAN).

As the initial experimental point, a first plate was measured 24h after plating and an arbitral value of 1 was assigned.

5. Flow cytometry

Actively growing cells were washed once with room temperature (RT) PBS and collected by centrifugation. For permeabilization, cells were incubated in cold ethanol at 4°C for 1 hour. They were washed in cold PBS and then, each cell sample was resuspended in the following mix: 300 µl de PBS at 4°C, 16 µl of 1 mg/ml ribonuclease A (Sigma) y 8 µl of 1 mg/ml propidium iodide (PI) (Sigma). PI is a DNA intercalation agent that becomes fluorescent when bounded to the DNA. Fluorescence is emitted in an estequiometric manner, being proportional to the amount of DNA in the cells. The cells were incubated in agitation in the dark at RT for 2 hours.

A dark and RT incubation in agitation was followed during 2 hours. Finally 10000 cells per sample (triplicates) were acquired FACScalibur (Becton Dickinson) using CellQuest software. Populations were selected by WinMDI software. Analyzing the histograms with WinMDI software we were able to calculate the population distribution in each cell cycle phase.

6. Protein extraction

Cell culture plates were placed on ice and were washed with 5 ml of 4°C PBS. Cells were resuspended in an appropriate (100-300 µl) amount of lysis mix: Cell lysis buffer 1x (Cell signaling), freshly supplemented with NaF 1mM, as a phosphatases inhibitor, PSMF and Complete (Roche), as proteases inhibitors. Cells were collected with a rubber policeman incubated on ice for 5' in microcentrifuge tubes and centrifuged at 12000 rpm for 10' at 4°C.

Protein concentration was measured by Bradford assay. We prepared a mix with 1µl of each sample, 800 µl milliQ water and 200 µl Bradford reagent (Bio-Rad) (duplicates) and mixed in a vortex for 20 seconds and incubated for 5' at RT. Absorbance at 595 nm was measured in a spectrophotometer (Ultrospec 2000, Pharmacia biotech).

7. Western blotting

Western blotting was performed with a SDS-PAGE Electrophoresis System (Bio-Rad). Between 20 and 50 µg of protein per sample were proportionally mixed with Laemmli buffer and denaturalized for 5' at 100 °C incubation. Then, the proteins in the samples were separated by electrophoresis through 7.5 to 12% Tris-HCl SDS-PAGE gels at 100-150 V until the gels were then transferred to nitrocellulose membranes using a semi-dry iBlot® system (Invitrogen). Finally, membranes were blocked in 2% BSA in TBS-T (20 mM Tris/HCl (pH 7,5), 150 mM NaCl and Tween-20 al 0.05%) from 30' to 2 hours. Next step was incubation with the primary antibody in 2% BSA in TBS-T at 4°C overnight or 2 hours at RT (Table 1).

Primary antibodies	Supplier	Origin	Dilution
P-ERK (Tyr204)	Santa Cruz	mouse	1:1000
ERK	Santa Cruz	rabbit	1:1000
P-Akt	HomemadeL15	rabbit	1:2000
Akt	Santa Cruz	rabbit	1:1000
P-p38 (Thr180/Tyr182)	BD	mouse	1:1000
p38	Santa Cruz	rabbit	1:1000
P-JNK (Thr183/Tyr185)	Cell Signaling	rabbit	1:1000
JNK	Santa Cruz	rabbit	1:1000
RasGrf1	Homemade L1	rabbit	1:2000
Pttg1	Immunostep	rabbit	1:1000
β-tubulin	Sigma	mouse	1:5000
CDK1	Santa Cruz	mouse	1:1000
Cyclin B	Santa Cruz	rabbit	1:500

Table 1. Primary antibodies used in Western blot.

After that time, membranes were washed four times for 5' at RT using 20 ml approx. of TBS-T in agitation. Then, they were incubated for 1 hour at RT with the appropriated secondary antibody (Table 2) diluted in blocking solution. We washed again four times for 10' at RT with TBS-T, and an Odyssey fluorescence scanner (LI-COR Bioscience) was used for detection. Quantification was performed using the scanner's software.

Secondary antibodies	Supplier	Origin	Dilution
Alexa Fluor® 680	Invitrogen	goat α-mouse IgG	1:10000
Alexa Fluor® 680	Invitrogen	goat α-rabbit IgG	1:10000
IRDye 800CW	LI-COR	goat α-mouse IgG	1:10000
IRDye 800CW	LI-COR	goat α-rabbit IgG	1:10000

Table 2. Secondary antibodies used in Western blot.

8. Luciferase reporter assays

pBK-CMV RasGrf1 containing the full-length RasGrf1 coding sequence, and the reporter plasmid construct pGL3-Pttg1 containing 2.3Kb from Pttg1 promoter region, were kindly supplied by Dr Lowy and by Dr Slomo Melmed [89] respectively. Cells were split into 12-well plates, and each well was cotransfected with Lipofectamine 2000® (Invitrogene) with a) 1µg luciferase promoter and hPTTG1 promoter and b) 1 µg empty pBK-CMV vector as control or 1µg pBK-CMV RasGrf1. pRL-Tk (Promega) encoding renilla luciferase was used as an internal control (5 ng/well) to normalize the transfection efficiency. 48 hours upon transfection, they were stimulated for 7h with the corresponding compound. Then, whole-cell lysates were collected for reporter detection by luciferase assays using a dual luciferase reporter kit (Promega, Madison, WI, USA).

- Nerve Growth Factor (NGF) 100 ng/ml (Promega)
- Ionomycin 500nM (Sigma)
- Epidermal Growth Factor (EGF) 100ng/ml (Peprotech)
- Lysophophatidic acid (LPA) 0.25 ng/ml (Sigma)
- U0126 25µM (Promega)
- Wortmannin 100nM (Sigma)
- SP600125 20µM (Calbiochem)

Reactions were measured using a Lumat LB 9507 Tube luminometer (BERTHOLD TECHNOLOGIES GmbH & Co. KG). Transfections were performed in triplicate and repeated in three independent experiments to assure reproducibility.

II. Second chapter of results

1. Animals

Ninety-eight C57BL/6J mice, weighing 170-340 g and between 12-14 weeks of age where used, 12 male and 11 female WT and 10 male and 9 female Pttg1 KO; 9 male and 6 female WT and 9 male and 5 female RasGrf1-Pttg1 KO; 8 male and 8 female WT and 6 male and 5 female RasGrf1 KO mice. Pttg1 KO mice were kindly supplied by Prof. Melmed [130]. RasGrf1 KO mice were generated at our lab as previously described [78].

Groups of animals with the same sex and genotype were housed in type IIL individually ventilated cages, in a temperature- and humidity-controlled room with a 12h light/dark cycle, with food (Teklad 2014, Harlan Laboratories) and water available ad libitum. All testing was completed during the light phase. Animal housing and experimentation followed the general recommendations of the European Communities Council Directive of 86/609/EEC and the RD 1201/05 about the use of experimental animals with scientific aims. Maximal efforts were made to minimize the total number of animals used as well as the suffering for them. The experimental procedures were approved by the local Animal Ethics Committee of the University of Salamanca.

2. Handling

Animals were handled daily for a period of five days during the pre-experimental period to reduce variations in their responses. The handling was executed by the researcher who was going to conduct the behavioral experiments.

3. Visual discrimination test

The visual discrimination test was used to check mice visual function. Each animal was placed for 5' in the four divided area table: with, stripped, checked and black (see Fig. 11 from Results). We measured the % of time spent on each area and how the animal passed from one to the next.

4. Behavioral experiment

The Barnes maze (Stoelting Europe) was a grey non reflective circular base plate (91cm diameter) with 20 holes (5cm) and an escape box under one hole. Cue density was low to moderate, consistent with previous rodent studies [136]. To reduce intra-maze odor cues, the maze surface and all the holes were cleaned with 70% ethanol between each session.

The week before starting the test handling was performed. Every day at the same hour each mouse was handled during one minute by the researcher to reduce stress during the behavioral test.

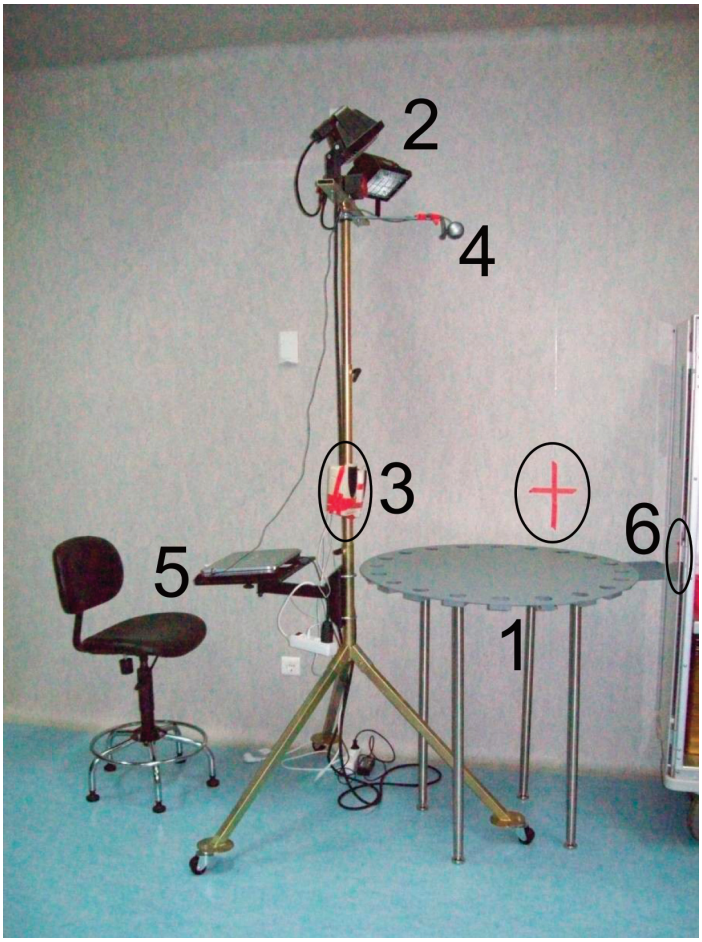

Fig 2. Barnes maze installation setup. **1.** Barnes maze table. **2.** Lights at the required high to achive 3000 lux (lumen/m^2) on the table. **3.** Speakers to apply 80 dB white noise during sessions. **4.** Webcam. **5.** Researcher location during sessions. **6.** Scape tunnel (open). During session it rests unseen under the table.

On the first testing day, mice were held in the escape box for 1 min, after which the first session began: Each mouse was placed in the center of the maze in an opaque white box. After 10 s the box was removed, a white noise buzzer (80 dB) and bright light turned on (3000 lux), and the mouse was free to explore. Sessions ended when subjects entered the escape tunnel or after 5 min had elapsed, whichever occurred first. Mice were tested once daily for 22 days. After a 12-day break, mice were tested on memory retention for 4 days. The reverse learning test began after the last day of memory retention testing, which entailed switching the target hole 180° from the original.

All sessions were recorded with a webcam and the following parameters were analyzed by Any-Maze software (Stoelting). The task yields measures of the following: latency to investigate the first hole, working memory errors, perseverations, distance from first hole explored to target hole (inclusive), total number of holes checked, and total time to escape. Working memory errors were those in which the mouse returned to a hole it had previously explored. Perseverations represented repeated sequential explorations of a hole (other than the target) or two adjacent holes.

Search strategies for each mouse's daily session were classified as the percentage of time spent using one of three defined categories [137]: (a) random search strategy: localized hole searches separated by crossings through the center; (b) serial search strategy: systematic hole searches in clockwise or counterclockwise direction; or (c) spatial search strategy: reaching the escape tunnel with both error and distance scores of less than or equal to 3.

5. Statistical analysis

The median of the data from four different time points was used. Data were analyzed by Friedman's ANOVA, with genotype-sex as a between-subjects factor and time as a within-subject factor. Wilcoxon signed-rank test was used as post hoc test. Mann-Whitney test was used to analyze significant differences between groups during a time point. Principal component analysis was also performed. All analyzes were done with SPSS program.

III. Third chapter of results

1. Animals

A total of one hundred seventeen C57BL/6J mice where used in glucose tolerance tests (GTT), weighing 148-320g. At three months of age, we used 7 male and 6 female WT and 12 male and 11 female double KO. At 10 months of age we used, 5 male and 4 female WT and 4 male and 5 female Pttg1 KO; 6 male and 6 female WT and 13 male and 13 female RasGrf1-Pttg1 KO; 4 male and 10 female WT and 6 male and 5 female RasGrf1 KO mice.

In order to establish the body mass phenotype, 23 non weaned pups for each group of C57BL/6J mice were used. These mice were also weighted after weaning. For the weaned pups groups, we used 42 male and 48 female WT and 26 male and 25 female Pttg1 KO; 30 male and 37 female WT and 39 male and 34 female RasGrf1 KO mice.

Glucose tolerance test mice weights were used for the three months and 10 months of age data.

Mice were housed in already mentioned conditions. This experimental procedure was also approved by the Bioethics Committee of the University of Salamanca.

2. Glucose tolerance test

We performed glucose tolerance tests on animals after a 14–16 h overnight fast. For these studies, glucose (2 mg of glucose per g of body weight) was injected intraperitoneally. After 15', 30' and 90' serum glucose levels were measured using a Glucometer ACCU-CHECK Sensor Comfort (Roche). We obtained blood for plasma insulin levels by submandibular blood collection in anesthetised mice by isofluorane (Schering Plough) inhalation [138]. Plasma insulin levels were measured by enzyme-linked immunosorbent assay (Rat/Mouse Insulin ELISA kit; Millipore).

3. Statistical analysis

To compare weights from two distinct groups we used t-student statistical test.

One-way ANOVA statistical test was used but when Levene's test was significant we used Welch statistical result. Bonferroni and Gabriel post hoc tests were used.

Results and discussion

I. Analysis of the signaling pathways involved in regulation of the Pttg1 expression by the RasGrf1 protein

1. Bioinformatics search of key proteins controlled by the RasGrf1 signaling pathways possibly involved in Pttg1 expression

In order to know if data from our RasGrf1 KO mice microarray studies and database analysis of the Pttg1 promoter gave us clues about the transcription factor probably involved in the regulation of Pttg1 expression by RasGrf1 we ran a bioinformatics analysis of the Pttg1 promoter, whose sequence and characterization were already published [139]. To this purpose we used TFSEARCH ver1.3, an online program that looks for highly correlated sequences in the TFMATRIX data base (see materials and methods).

From this analysis came out 36 transcription factor consensus sequences (Table 3) using the 2.3 kb suggested as promoter sequence for Pttg1 [139].

AML-1a	E2F	HSF2	RORalp
Brn-2	E4BP4	Ik-2	S8
CdxA	Elk-1	Ik-3	Sox-5
C/EBP	Evi-1	Lyf-1	Sp1
C/EBPb	GATA-1	MEF-2	SRY
c-Ets	GATA-2	MZF1	TATA
COUP-T	GATA-3	Nkx-2	USF
CP2	HFH-1	NRF-2	v-Myb
CRE-BP	HNF-3b	Oct-1	YY1
deltaE	HNF-4	Pbx-1	

Table 3. 36 transcription factor consensus sequences using 2.3 kb Pttg1 promoter sequence.

Next step was the use of Cytoscape, another bioinformatics program, and its plugin, APID2NET (see materials and methods), to investigate the RasGrf1 interactome, limiting it to 4 connection levels and at least one experimental method for each proposed interaction. From the RasGrf1 interactome we obtained 1457 proteins and from the 36 transcription factor list (Table X) 669 proteins. Then we compared both lists and we obtained 159 proteins, all of them candidates to be the nexus between RasGrf1 expression/activity and Pttg1 expression (Table X, supplementary material).

Then, we compared these 36 transcription factors with the transcription factors showing altered expression in the microarrays analysis of RasGrf1 KO mice retina and β-cells (Affimetrix MOE 430A mouse Gene Chips). We found three coincidences in the β cells list and nine in the retina (Table 4).

WT versus KO for RasGrf1			
β cells array		**retina array**	
Aebp2	Ftsj1	**Pit1**	COMP1
Ankrd10	Jund1	PPAR	Cdx-2
Brd4	Nr3c1	XFD-2	TCF-4
Btg2	Phtf1	CDX	**E2F-4:DP-2**
Cbfb	Plagl1	**PBX**	**E2F-1:DP-2**
Cul3	Pnrc1	Cdc5	**E2F-1:DP-1**
Ddit3	Smc4l1	**GR**	Imperfect
Egr1	Supt4h1	TTF1	Hogness/Goldberg
Fosb	Tcf4	E47	BOX
Foxa2	Rmpo	**NF-1**	Major T-antigen
Foxp1	Zhx1	HNF-1	**AR**
		MEF-2	**MyoD**
		Nrf-1	

Table 4. Altered expression transcription factors in the microarrays analysis of RasGrf1 KO mice. Coincidences highlighted in black.

There are evidences that the MAPKs pathway control over Egr1 (early growth response 1) expression. It has been described that the ternary complex factor (TCF) Elk-1, is a link between Raf/MEK/ERK and SFR-dependent genetic transcription [140, 141]. It has been confirmed a link between serum response element (SFR) and the transcriptional regulation of Egr1 [142]. Still, there are two MAPKs related to mechanical stress, p38 and JNKs, that also induce Egr1 expression [143]. It is interesting to point out that the expression of this transcription factor is altered by insulin in adipocytes 3T3-L1 resistant to insulin [144]. Egr1 induction requires ERK-dependent microRNA-191 downregulation and ERF (ETS2 repressor factor) phosphorylation, that leads to its exclusion from the cell nucleus [145].

FosB is a known target of the Ras/ERK pathway activation [146]. It has been recently published that in mammary human cells, while EGF induces Egr1 and it is necessary for migration, c-Fos and FosB increase serum dependent proliferation [145]. In 5' flanking region of this gene it has been identified several consensus sequences, among them SRE and AP-1 binding sites [147].

In 2009, RasGrf1 expression was directly correlated with β cells proliferation [148]. Calcium channels L-type and Glp-1 receptor agonists induce proliferation in the mouse insulinoma cell line, R7T1. The microarray analysis of these cells shows that *RasGrf1* is among the upregulated genes, and Egr1 and FosB among the transcription factors. Very interesting data regarding FosB in RasGrf1/Ras/ERK signaling has been described by Fasano et al. In this study they analyze the long-term responses to cocaine in RasGrf1 KO mice, showing a role for the RasGrf1/ERK/FosB axis in the control of striatal networks in response to the stimuli.

A good example of the relevance of FoxA factors in multiple developmental stages of the same cell type is the pancreas. Foxa1/Foxa2 activate Pdx1, the most important gene responsible of pancreatic development [149]. Additionally, these two factors cooperate in the control of insulin secretion of mature β cells and are repressors of neuronal transcription by a mechanism yet unknown [150]. In view of these publications, alterations in the expression levels of Foxa1 and Foxa2 may be a reflect of the downregulation of MAPKs signaling in RasGrf1 KO mice.

Pit-1 is a pituitary transcription factor, key in cell differentiation during anterior pituitary organogenesis [151, 152] and as pituitary transcription activator [153]. Pit-1 activates growth hormone (GH) transcription and induces proliferation in normal and tumorous human breast [154]. In RasGrf1 KO mice, reduced GH circulating levels have been described, which may reflect this transcription factor altered expression [76].

Retinoblastoma (Rb) protein interacts with E2F transcription factors to control G1/S cell cycle transition and allow proliferation. DP heterodimers association to E2F regulates binding to its targets, like cyclins D1 and E, c-myc, and cdc2, whose products are necessary for the nucleotide synthesis, DNA replication and cell cycle progression. In Rb+/− mice there is an increase in E2F1 and Pttg1 expression in pituitary and in human pituitary tumors it also exists a correlation between them. It has already been confirmed the binding of E2F1 to the Pttg1 promoter and the activation of transcription. Therefore, aberrant activation of Rb/E2F1 pathway may induce Pttg1 exaggerated expression, leading to an unreliable sister chromatids separation [84], chromosomal instability [155], loss of proliferative control [124] and, as consequence, beginning of the oncogenic process [156].

2. Functional characterization of shRasGrf1 and shPttg1 stable PC12 clones.

PC12 cells were chosen for the in vitro experiments because of their extense bibliography in neurobiological and neurochemical studies since this cell line was established more than 30 years ago [157]. Moreover, its neuronal origin could simplify the comparison between the results obtained with them and the previous from mice retina, where we first observed a relation between RasGrf1 and Pttg1 [158].

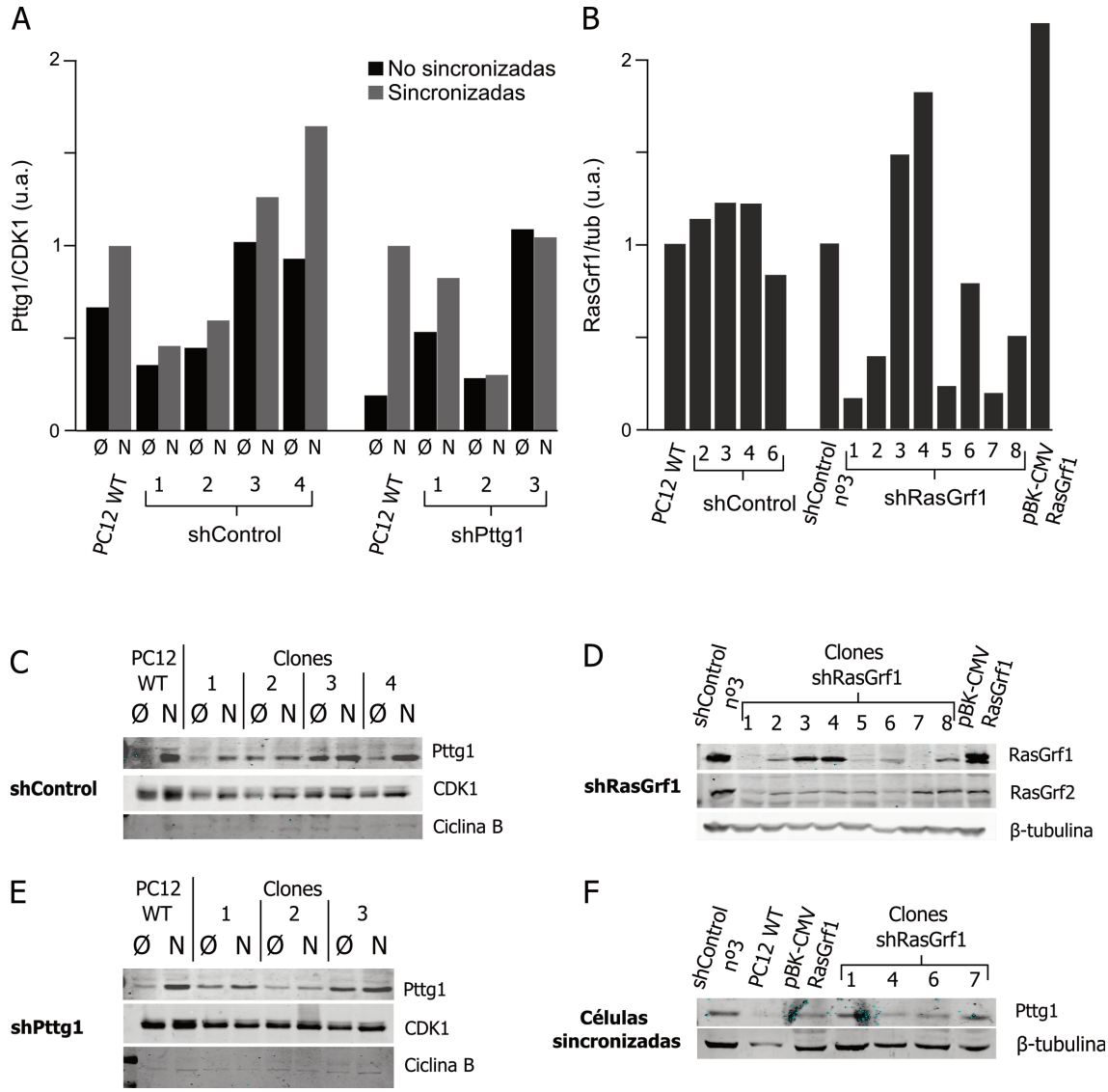

Fig 3. RasGrf1 and Pttg1 silenced PC12 cells by shRNA stable silence. **A.** Representative bar-plot in **C** and **E** Western blots. **B.** Representative bar-plot in **D** Western blots. Tub, β-tubulin.

a. RasGrf1 and Pttg1 effect in PC12 cells proliferation.

MTT cell incorporation was the technique used in the proliferative assays. This procedure allows the indirect measurement of the cells growing rate by the analysis of their mitochondrial activity of proliferative cells. We have not observed changes the metabolic state of any of the clones.

After the analysis of the results we observe a clear decrease in the growth of the shRasGrf1 clone, while the overexpressed RasGrf1 clone shows a slight increment in proliferation level (fig 4 B). shPttg1 clones proliferate a little faster than the control ones (fig 4 A).

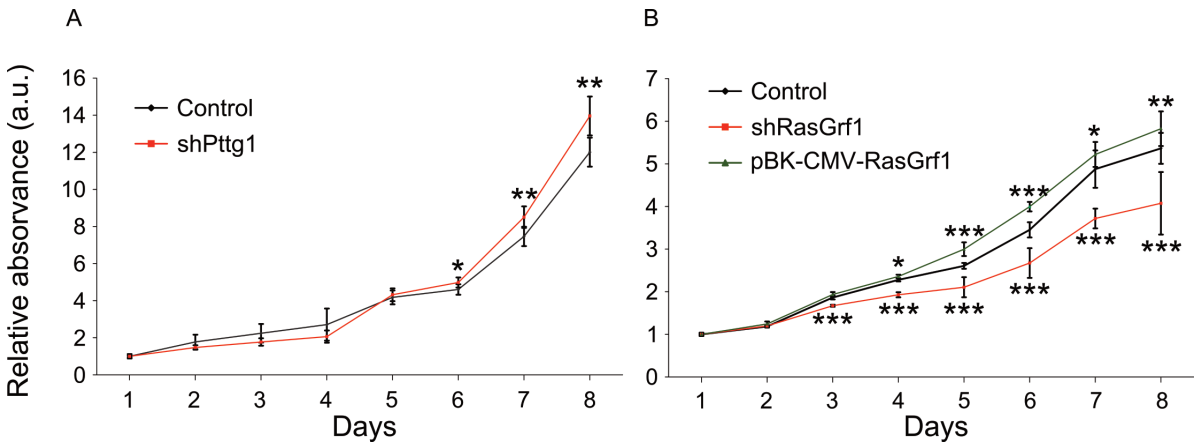

Fig 4. Proliferation rates of PC12 clones expressing shPttg1, shRasGrf1 and pBK-CMV-RasGrf1 as measured by the MTT incorporation assay. Absorbance values are expressed in relative units. Initial point was set at 24 hours after plating the same number for cells of each clone and its absorbance was taken as reference. Each point represents the media of the relative absorbance of triplicates. Control, shControl clones and pBK-CMV vector. The error bars represent ± SD. *, p<0.05. **, p<0.01. ***, p<0.001 in comparison with Control (t-test).

The only proliferation study found with downregulated Pttg1 expression by siRNA (short interference) was done also using the MTT assay, but in human hepatocarcinoma HepG2 and SMMC-7721 cell lines [159]. In contrast to our results, a great decrease in proliferation rate was observed. We expected an increase of the growth rate because of the known role of Pttg1 in the anaphase checkpoint and its possible relaxation upon a downregulation in Pttg1 expression. This fits with the moderate increase in proliferation that we observed in our PC12 model. In overexpression experiments there is also controversy, in NIH3T3 and HEK 293 has been described an increase in proliferation [122] and an inhibition in HeLa an A549 cells [114, 160]

b. Cell cycle analysis of the shRasGrf1 and shPttg1 stable clones.

With the proliferation results in mind, we thought that the cell cycle might be altered in these clones where proliferation was changed. We used flow cytometry studies to analyze the cell cycle in growing cells. The results confirmed that these proteins play a key role in mitosis regulation of the PC12 cell. In the dot plots and in the histogram we could observe a clear chromosomal instability (CIN) in the shRasGrf1 and shPttg1 clones with a high percentage of cells showing a chromosome rate higher than the control or the WT cells.

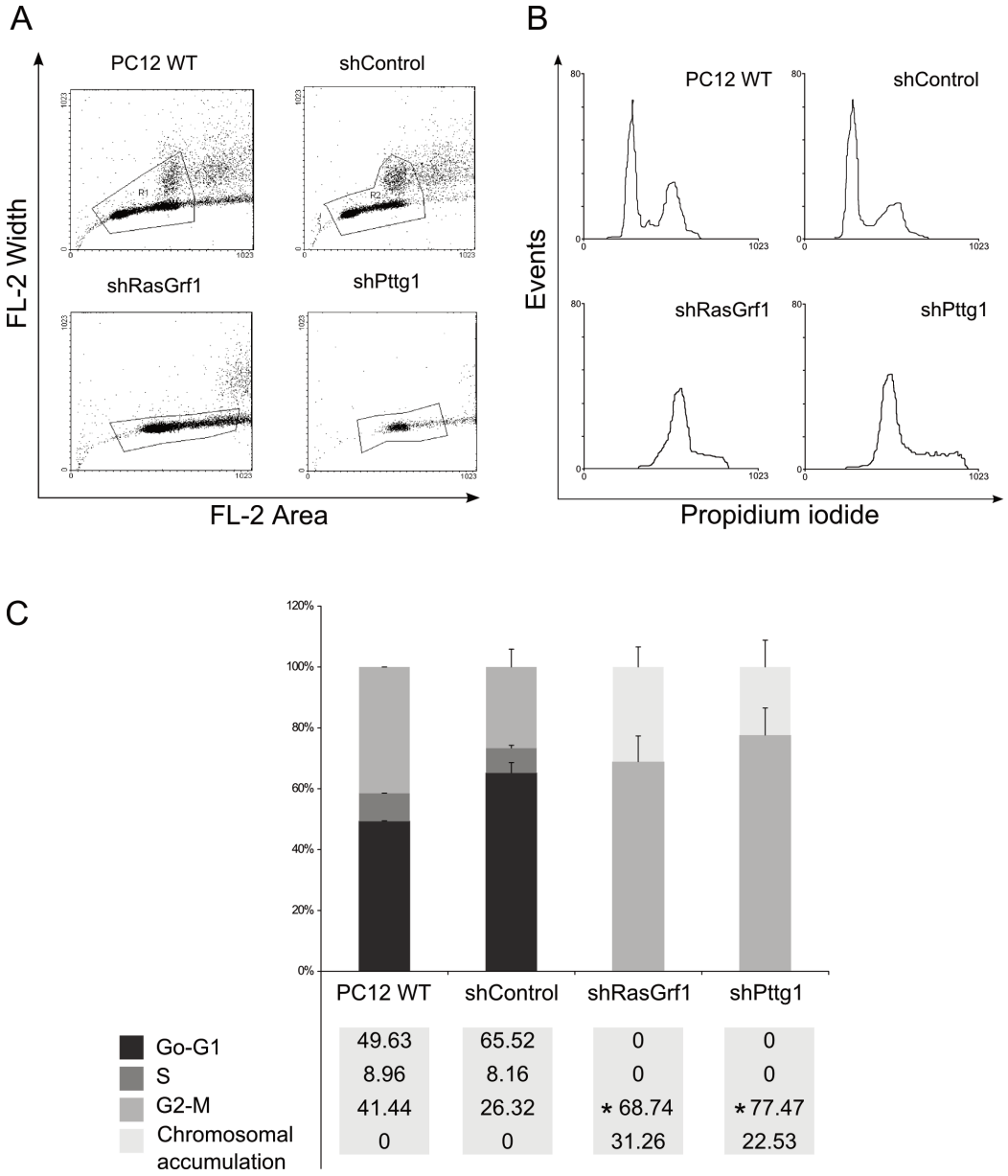

Fig 5. Study of the cell cycle in the shRasGrf1 and shPttg1 stable clones. Cell cycle profile of the shRasGrf1, shPttg1, shControl clones and uninfected PC12 cells. **A.** Representative dot-plots of each clone. FL-2 Width, cell size. FL-2 Area, cell internal complexity. **B.** Representative histograms of propidium iodide fluorescence emission for each clone. **C.** Bar-plot represents the mean of three independent experiments of the cells percentage in each cell cycle phase. Error bars represent ± SD. * $p<0.05$ (t-test).

The CIN describes an increment in the rate of defective segregated chromosomes in mitosis, provoking a fail in the maintenance of the correct chromosomal complement (euploidy). Aberrant chromosomal state is classified by changes in the ploidy, complete chromosome gain or loss (aneuploidy) or main chromosomal rearrangements (GCR), all of them typical of solid tumors. Multiple mechanisms related to chromosomal segregation may cause CIN: a checkpoint of the mitotic spindle assembly too weak or too strong, defective cohesion of sister chromatids, merotelic binding increased kinetochore-microtubules or the presence of extra centrosomes. It has always been proposed that CIN promoted tumor progression, however there are studies suggesting a promotion or a suppression of tumor progression depending on the context [161].

Mitotic spindle assembly checkpoint (SAC) is a signaling pathway that assures the correct segregation of the sister chromatids inhibiting metaphase-anaphase transition until all the chromosomes are integrated to the mitotic spindle [162]. APC/C complex, E3 ubiquitin ligase, targets mitotic regulators for its degradation allowing chromosomal segregation [163, 164]. CDC20 is an APC/C key cofactor in this pathway. It targets PTTG1 and cyclin B when binding to the spindle is achieved [165].

A detailed analysis of altered genes in tumors shows a high enrichment on centrosomal and mitotic genes in its expression profile [166]. CDK1 and some of its upregulators, cyclin B1 and B2, CKS1 and 2 were upregulated. CIN profile includes additional components to the centrosomal and chromosomal segregation machinery: NEK2, aurore kinase A, aurore kinase B, CDC20, CDCA8, CENPF, separase (codified by ESPL1), hPTTG1, TTK and MAD2L1 [167]. CIN tumors usually overexpress centrosomal proteins like CDK1, cyclins E, A and B, in addition to RasGrf1, NEK2, Aurora kinasa A, PLK1 o TPX2 [167, 168].

Finally, I would like to mention Yu et al. results using mouse insulinoma cell line MIN6, similar to the BTC3 cells that we have used for Pttg1 promoter luciferase assays. Slight overexpression of Pttg-EGFP led to its degradation two minutes before the transition metaphase-anaphase. In contrast, when it is abundantly overexpressed, this transition stops, cells are not able to degrade it and some of them enter apoptosis (≈18%) [169].

c. Effect of the RasGrf1 and Pttg1 downregulation in PC12 cells on Ras signaling pathways.

To examine the state of the signaling pathways activated by RasGRf1 in PC12 cells with diminished expression of Pttg1 or RasGrf1 we used three well-known compounds, two of them known RasGrf1 activators.

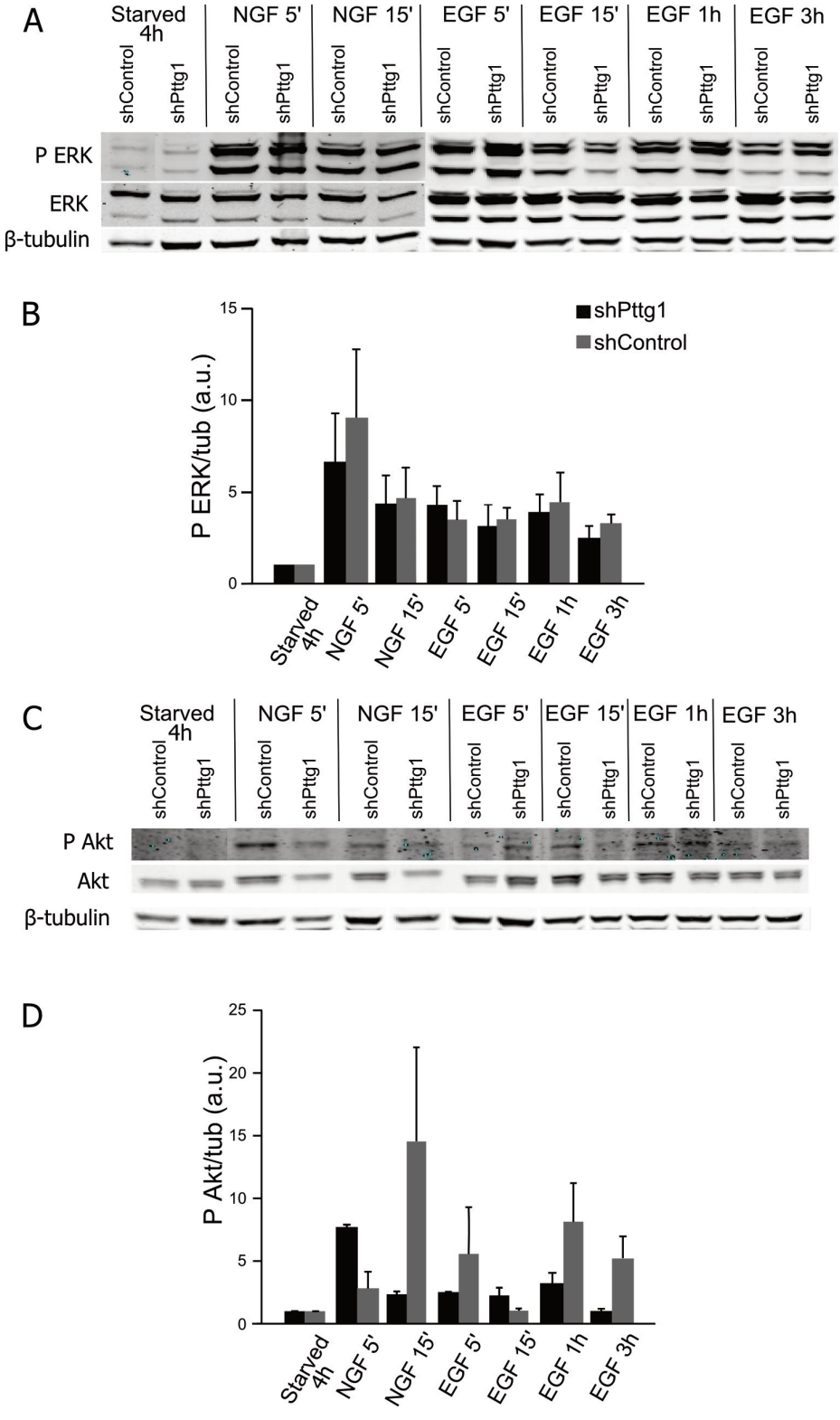

Fig 6. ERK1/2 and Akt phosphorylation in shPttg1 and shControl PC12 clones. After 4h starvation in sub-confluent cell cultures, we stimulated with NGF (100ng/ml) or EGF (25 ng/ml) during the indicated times. Representative Western blots showing the phosphorylation of **(A)** ERK1/2 and **(C)** Akt phosphorylation levels. Error bars represent the mean of 4 independent experiments using one shControl clone and two shPttg1 clones for ERK1/2 **(B)** and 2 independent experiments using two shControl and two shPttg1 clones for Akt **(D)**. β-tubulin (tub) expression used to normalize.

NGF (nerve growth factor) binds TrkA (tropomycin-related kinase A) receptor, provokes its dimerization, phosphorylation and the stabilization of its active conformation. It allows Shc binding to the receptors and recruit Grb2 and Sos, a Ras GEF, to the membrane. Sos interacts with its Ras target and activates MAPKs pathway [170-172]. TrkA also activates RasGrf1 through interaction through its HIKE domain, resulting in RasGrf1 phosphorylation and an increase in neurites growth [35].

Ionomycin is an calcium ionophore widely used in PC12 cells [173]. Arozarena et al. (2004) suggest that, in COS-7 cells, intracellular calcium stimulation by ionomycin produce RasGrf1 and RasGrf2 dependent H-Ras activation in the plasma membrane [14].

EGF (Epidermal Growth Factor) stimulates cell growth, proliferation and differentiation by binding to its receptor [174]. EGF does not activate RasGrf1, but it does activate the ERK pathway [28], so we used it as a positive control of the experiment.

The results obtained using shPttg1 clones, as expected, do not show any significant changes when compared with shControl in ERK nor in Akt pathway activation. In fig. B we can appreciate some difference between shPttg1 and shControl clones due to variability, as we can see in the error bars. We think that other factors independent of the Pttg1 of expression must be influencing in Akt phosphorylation, Pttg1 expression independent.

In shRasGrf1 clones study we were interested in the state of the MAPKs pathways: ERK, JNK, p38, but also in the PI3K/Akt pathway, because of its integration with the Raf/MEK/ERK pathway [175]. The knowledge of the pathways altered by overexpression and downregulation of RasGrf1 will let us focus in those pathways more probably involved in RasGrf1 regulation of Pttg1 expression.

There are no significant differences in P-Akt (C), P-JNK (E and F) or P-p38 (G and H) at short term with the stimulus used. This is not totally unexpected for the JNK and p38 MAPKs, since they are usually activated by stress signals. If we observe ERK (B) and Akt (D) with pBK-CMV-RasGrf1, we appreciate a subtle trend towards a difference to be more phosphorylated in a RasGrf1 independent manner, although with no statistical significance.

We find statistically significant differences in P-ERK levels in the shRasGrf1 clones. EGF stimulation, even being RasGrf1 independent, is increased. A possible explanation could be that RasGrf1 has a role in modulating the phosphorylation intensity of the pathway. NGF stimulation showed us again unexpected increase in ERK phosphorylation in RasGrf1 silenced clones. Finally, ionomycin stimulation also moderately increased ERK phosphorylation, but only at 5'.

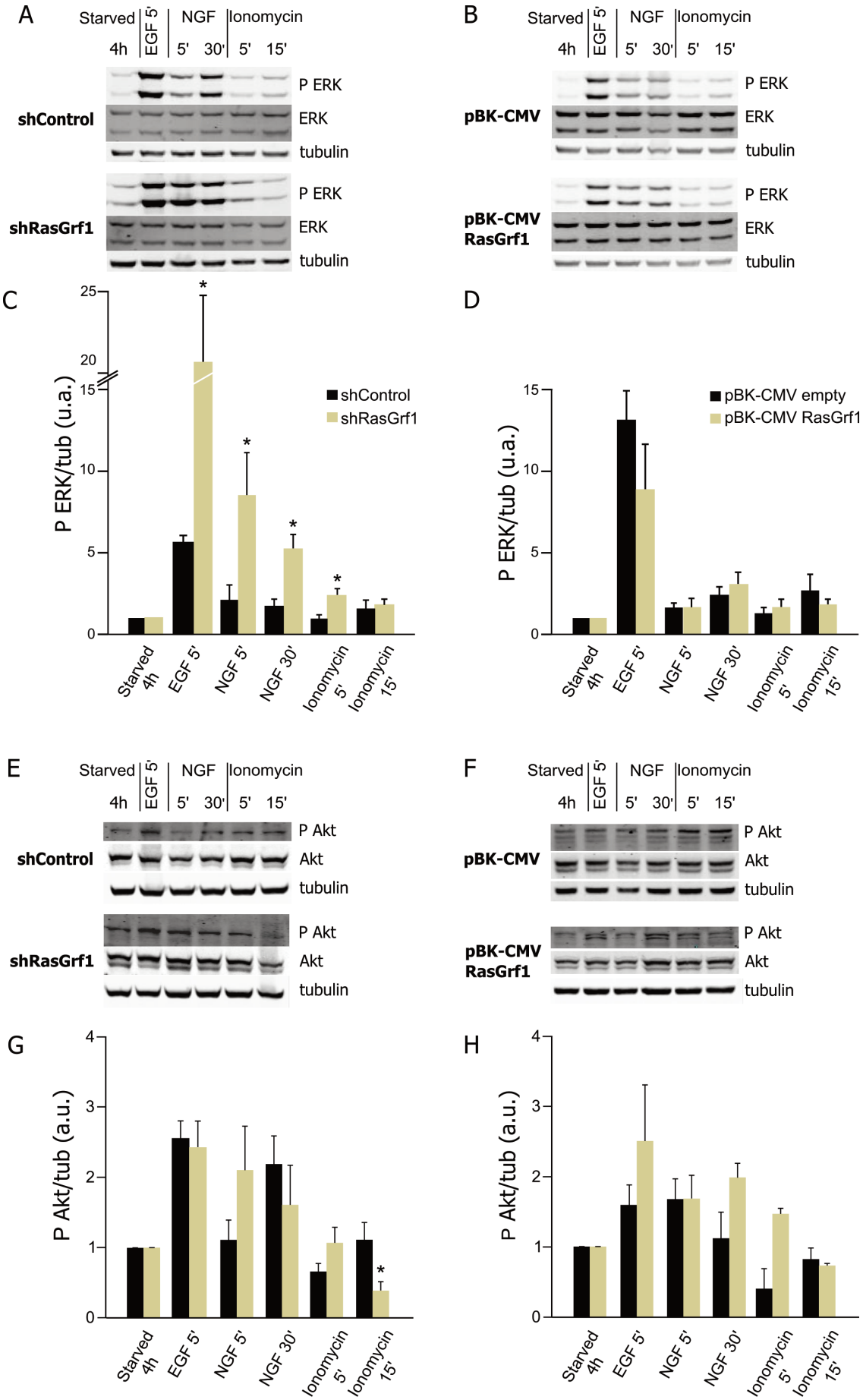
A
Starved
4h
EGF 5'
NGF
5'
30'
Ionomycin
5'
15'
shControl
P ERK
ERK
tubulin
shRasGrf1
P ERK
ERK
tubulin
B
Starved
4h
EGF 5'
NGF
5'
30'
Ionomycin
5'
15'
pBK-CMV
P ERK
ERK
tubulin
pBK-CMV RasGrf1
P ERK
ERK
tubulin
C
P ERK/tub (u.a.)
25
20
15
10
5
0
shControl
shRasGrf1
Starved 4h
EGF 5'
NGF 5'
NGF 30'
Ionomycin 5'
Ionomycin 15'
D
P ERK/tub (u.a.)
15
10
5
0
pBK-CMV empty
pBK-CMV RasGrf1
Starved 4h
EGF 5'
NGF 5'
NGF 30'
Ionomycin 5'
Ionomycin 15'
E
Starved
4h
EGF 5'
NGF
5'
30'
Ionomycin
5'
15'
shControl
P Akt
Akt
tubulin
shRasGrf1
P Akt
Akt
tubulin
F
Starved
4h
EGF 5'
NGF
5'
30'
Ionomycin
5'
15'
pBK-CMV
P Akt
Akt
tubulin
pBK-CMV RasGrf1
P Akt
Akt
tubulin
G
P Akt/tub (a.u.)
4
3
2
1
0
Starved 4h
EGF 5'
NGF 5'
NGF 30'
Ionomycin 5'
Ionomycin 15'
H
P Akt/tub (a.u.)
4
3
2
1
0
Starved 4h
EGF 5'
NGF 5'
NGF 30'
Ionomycin 5'
Ionomycin 15'

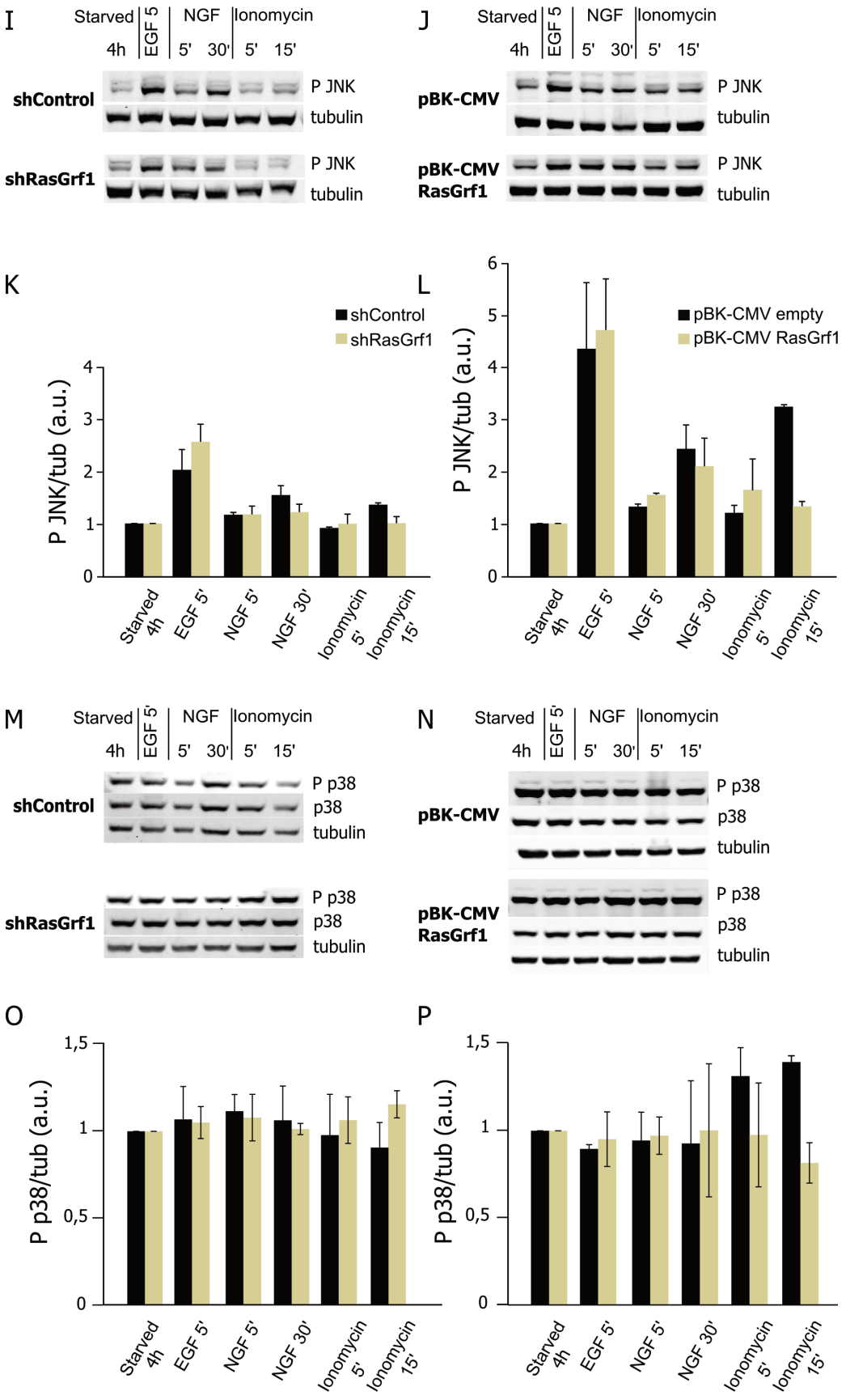

Fig 7. ERK1/2, Akt, JNK and p38 phosphorylation in shRasGrf1, shControl and pBK-CMV RasGrf1 and its control. After 4h starvation of subconfluent cell cultures, we stimulated with NGF (100 ng/ml), EGF (25 ng/ml) or ionomycin (100 nM) during the indicated times. Error bars represent the mean of 3 independent experiments using one clone for pBK-CMV, pBK-CMV RasGrf1 and shControl and two clones for shRasGrf1 in the ERK1/2 and Akt analysis and from two independent experiments using one clone pBK-CMV, pBK-CMV RasGrf1 and shControl and two shRasGrf1 for JNK and p38. Error bars represent + ET. * $p<0.05$ (t-test).

3. Study of RasGrf1 signaling dependence of Pttg1 promoter activation.

After concluding with the previous experiment that ERK pathway was the only one altered by RasGrf1 downregulation, we wondered if this pathway was also the only one able to modulate Pttg1 promoter activity. For that purpose, we carried on luciferase assays, transfecting a plasmid containing Pttg1 promoter next to the luciferase reporter and cotransfecting PBK-CMV-RasGrf1 construction or the empty vector. In all cases a vector containing Renilla was also cotransfected to normalize.

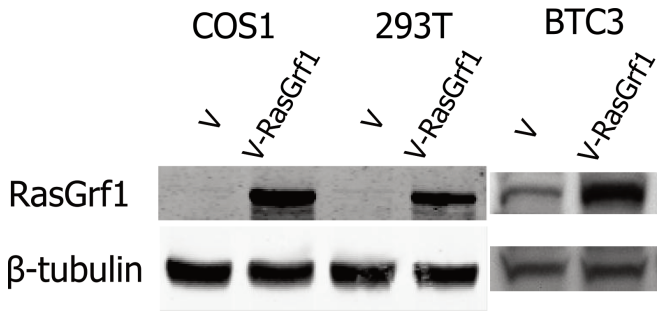

Fig 8. Representative Western blots of RasGrf1 overexpression in COS1, 293T y BTC3 cell lines. V, pBK-CMV.

RasGrf1 overexpression produces different effects on the control of the Pttg1 promoter depending on the cell line examined. COS1 and 293T cells, where RasGrf1 is not expressed, its overexpression reduces promoter activity. A more detailed analysis showed us that ionomycin and LPA induction do induce a 50% increase in Pttg1 promoter activity upon RasGrf1 overexpression when compared with unstimulatedRasGrf1 cotransfected samples. In contrast, EGF did not modify promoter activity. Regarding 293T cells, we do not observe increases in Pttg1 promoter activity with any of the compounds tested in this analysis.

Regarding the luciferase assay using specific inhibitors, MEK1 inhibition using U0126 reduced ≈50% promoter activity in all cell lines, while was not possible to extract a conclusion with the other inhibitors. This result points to a specific role of ERK pathway in the control of Pttg1 promoter activity.

As COS1 and 293T are easily transfected cell lines they have been widely used in signaling studies. However, they are not the best model to investigate the role of RasGrf1 because it is not naturally expressed in them. That is why we performed the assays in PC12 cells and in the mouse insulinoma cell line BTC3. The results obtained were less surprising than the previous ones. In BTC3 cells, although inductors did not change Pttg1 promoter activity, RasGrf1 overexpression increased it in a 30%. As observed before with the other cell lines, the only inhibitor that affected Pttg1 promoter activity in PC12 cells was MEK1 inhibitor U0126.

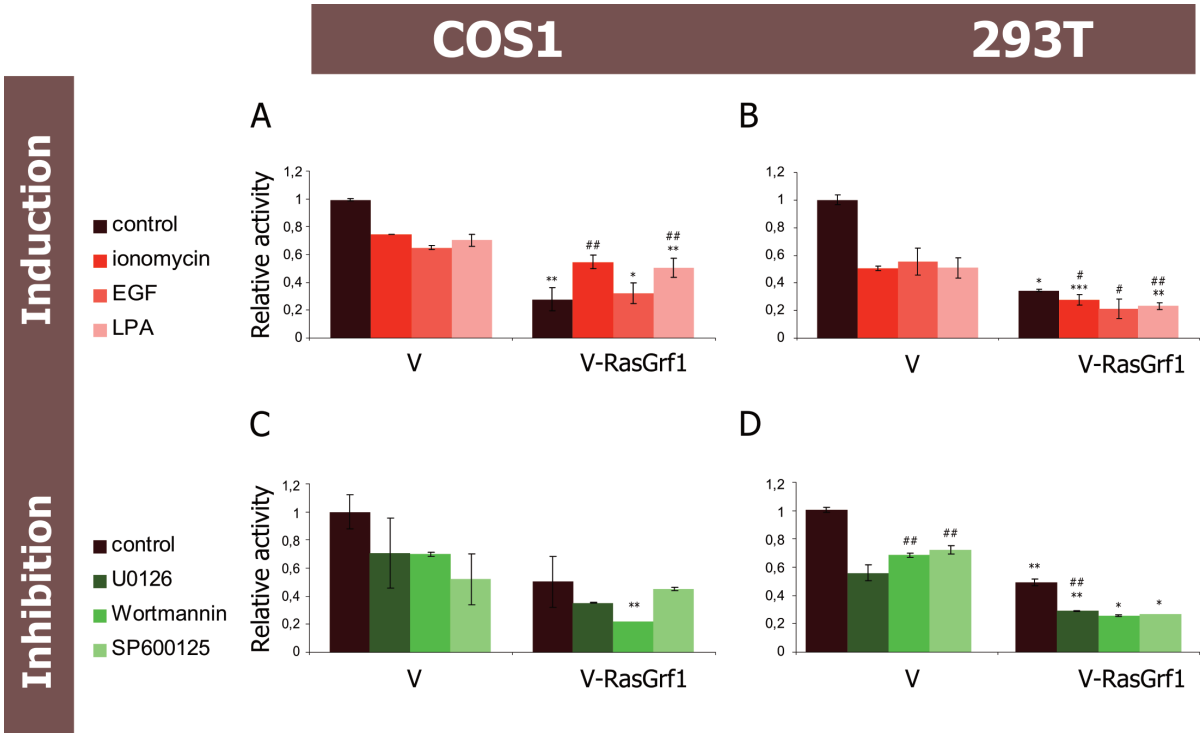

Fig 9. Luciferase assay measurement of Pttg1 promoter activity using COS1 and 293T cell lines. All inductions and inhibitions lasted 7 hours in cells transfected 48 hours before. * p<0.05, **p<0.01, ***p<0.001 comparing to the same stimulus without RasGrf1 overexpression. # p<0.05, ## p<0.01, ### p<0.001 comparing to the RasGrf1 overexpressed non stimulated control sample. V, pBK-CMV.

Finally, we analyzed NGF effect on the Pttg1 promoter activity in PC12 cells, as we already have studied its influence in the signaling pathways. We found significant differences between shControl and shRasGrf1 clones, where the promoter activity dropped in a 75%. Surprisingly, we do not observe an increase in luciferase activity when overexpressing RasGrf1, although a strong increase in the activity (90%) was obtained in this RasGrf1 overexpressing cells upon NGF stimulation.

Our results suggest that the ERK signaling pathway has a role in controlling Pttg1 promoter activity in all cell lines examined. This control is determined by RasGrf1 dependent Ras activation in BTC3 and PC12 cells, where RasGrf1 is expressed. Meanwhile, in COS1 and 293T cell lines, although ERK activation is still necessary, another Ras GEF must be responsible of the promoter activity regulation. The effect of MEK activity in Pttg1 promoter activity regulation may be important in the misregulated Pttg1 expression found in tumors.

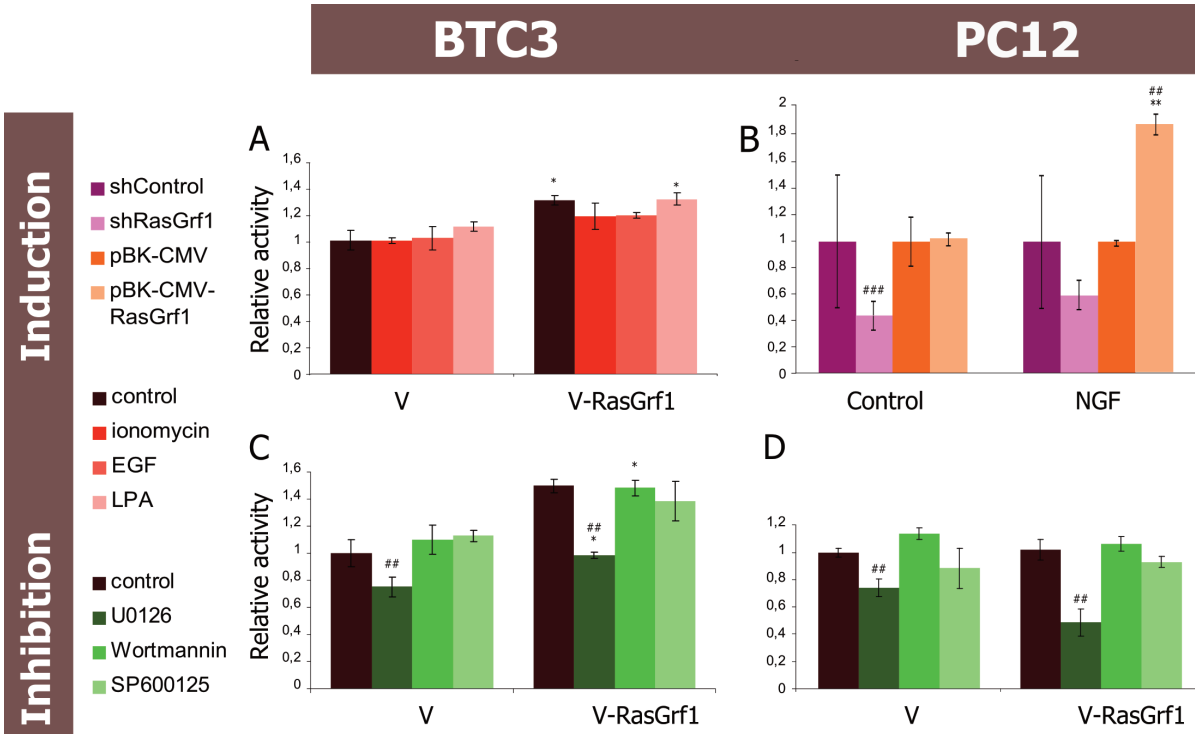

Fig 10. Luciferase assay measurement of Pttg1 promoter activity using BTC3 and PC12 cell lines. All inductions and inhibitions lasted 7 hours in cells transfected 48 hours before. * p<0.05, **p<0.01, ***p<0.001 comparing to the same stimulus without RasGrf1 overexpression. # p<0.05, ## p<0.01, ### p<0.001 comparing to the control sample of the same condition.

II. The role of RasGrf1 and Pttg1 in learning and memory

One of the specific aims of this thesis has been to investigate if Pttg1-/- mice had impaired hippocampal functions. This protein is abundantly expressed at the hippocampus, as observed in situ hybridization at the Allen Institute for Brain Science (brainmap.org). If a phenotype was observed we were also interested to analyze whether it was worsened in RasGrf1-/--Pttg1-/- mice. We also wanted to check if the RasGrf1-/- generated in our laboratory had impaired spatial memory like that observed in Giese et al. mice [68] or whether they behaved as the mice described by Brambilla et al. [67]. Previously, we have analyzed the hippocampal structures of the three genotypes using hematoxylin-eosin stained slides from the brain (data not shown). We did not appreciate any differences between de KO hippocampus and their controls. It has already been published that our RasGrf1 KO mice line has no hippocampal structural defects [158].

In this chapter we study the spatial memory of the genotypes above mentioned, using Barnes circular maze [137, 176]. In addition, the protocol used allows us to measure of aspects regarding both reference and working memory within the same test session [177].

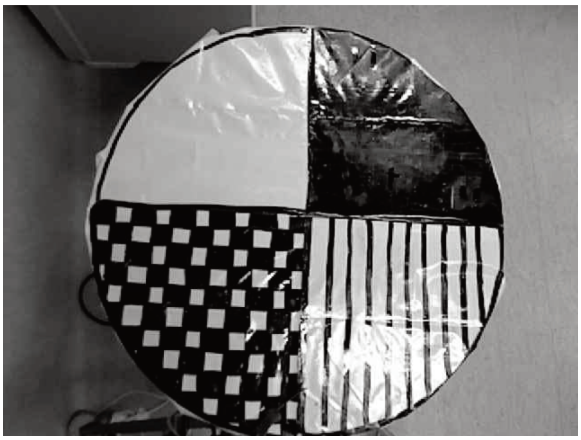

Fig 11. Plastic cover with four different areas to analyze the mice visual discrimination capacity.

Previously, to be sure that the mice had no visual problems, we used an easy experiment of black and white visual discrimination. We prepared a plastic cover with four different areas (Fig). Mice were placed one by one in the middle covered by an opaque box for 10 seconds. Then lights were turned on (3000 lux) and the mouse was released to explore the table during 5 minutes. All mice showed a clear preference for the total black and the black and white checker areas. When they explored a zone limit for the first time, all of them were cautious and tried to cross slowly. We did not observe differences in the performance between mice phenotypes nor sex.

1. Principal component analysis

In order to start the analysis of the large amount of data recorded during the Barnes maze test, it is critical to use statistics that include multivariate analysis. Variables located in the same quadrant of the PCA score plot are positively correlated to one another. Varia-

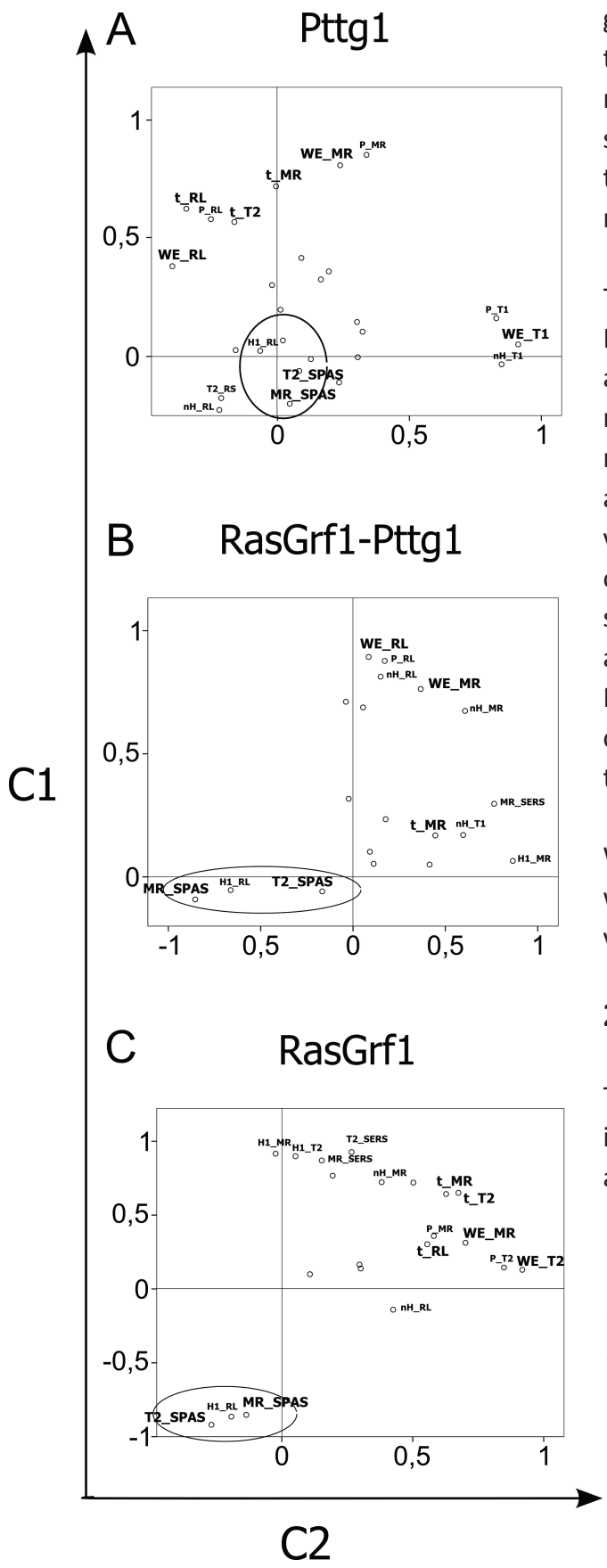

bles located in opposite quadrants are negatively correlated to one another. The distance of the variable from the origin is related to the deviation from the average, so this last premise was used to identify the most affected variables by mice genotype and sex.

These representations show us that the PCA score plots (Fig.) have a similar appearance for RasGrf1 (C) and RasGrf1-Pttg1 mice. In contrast, Pttg1 variables (A) are more dispersed in the score plot quadrants and the influence between each other is very different to that observed for the other two genotypes. As they lay in the same quadrant, circled variables show an analogous behavior of the RasGrf1 and RasGrf1-Pttg1 KO mice compared to their control groups, meanwhile the rest of them are located in the +,+ quadrant.

We have chosen the total time, number of working errors and spatial search strategy variables for a deeper analysis.

2. Total time

Total time needed to finish the task give us information of the learning level achieved and its quality. Maximal time to explore

Fig 12. Score plots of the three PCAs performed. C1, first component. C2, second component. Variables: t, total time. WE, working errors. SPAS, spatial search. P, perseverations. nH, number of holes explored. Periods: T1, first four learning days. T2, last four learning days. MR, memory retention. RL, reverse learning.

and find the escape hole is 300 seconds, then the mouse is driven by the researcher to the escape hole, helped to enter and kept in it for 30 seconds with no light neither noise. We have observed that sometimes the mouse runs to the escape hole but, instead of entering, it steps several times in it and in the contiguous one until it decides to enter. We think that maybe it does not remember well if it was the good hole or, that it wants to be sure that the hole is safe before jumping inside.

We have not found significant differences between the WT and the KO RasGrf1 males and females. The four groups studied for this genotype learned to finish the task and we see that in the significant differences found between periods for the same group: WT males $\chi2(3)=0.266$, $p<0.05$; WT females $\chi2(3)=0.013$, $p<0.05$; KO males $\chi2(3)=0.001$, $p<0.05$; KO females $\chi2(3)=0.007$, $p<0.05$. Wilcoxon test used as post hoc test shows no significant differences, but even without them we can see a considerable improvement of WT female and KO male from T1 to T2 and of the two WT groups and KO male from T1 to MR.

This result matches very well with Raffaele d'Isa et al. recently published work [178]. After ten years of controversy, they have finally demonstrated that RasGrf1 KO mice have no spatial memory defects, but impaired contextual fear conditioning. In this study they used the GENA53 mouse line, in which a non-sense mutation was introduced in the RasGrf1 coding region without additional changes in the genome. To explain the different spatial learning phenotype found between Giese et al. [68] and Brambilla et al. [67] mouse lines, d'Isa et al. attribute these differences to genomic alterations produced as a consequence of the different position of the mutation within the RasGrf1 locus and/or the insertion of the neomycin resistance cassette.

We do not appreciate significant differences between RasGrf1-Pttg1 WT and KO mice but we do when we compare the same group for different periods showing that both genotypes learned the task correctly. WT males $\chi2(3)=0.030$, $p<0.05$; WT females $\chi2(3)=0.000$, $p<0.05$; KO males $\chi2(3)=0.006$, $p<0.05$; KO females $\chi2(3)=0.011$, $p<0.05$. In the post hoc test just WT females show a significant difference from T1 to T2, from T1 to MR and from MR to RL. From T2 to MR the difference is close to be significant, pointing for a better consolidating process than the other groups.

Total time spent by Pttg1 mice shows significant differences between periods for each group, but also between groups in the same period. Between periods, Friedman's ANOVA give us the next significances: WT males $\chi2(3)=0.000$, $p<0.05$; WT females $\chi2(3)=0.000$, $p<0.05$; KO males $\chi2(3)=0.002$, $p<0.05$; KO females $\chi2(3)=0.001$, $p<0.05$. The post hoc test confirms us that all the groups improved their total time from T1 to T2, but no one from T2 to MR. Kruskal-Wallis test shows us that differences between female groups are statistically significant at T2 and almost significant at MR. Pttg1 male groups data were si-

milar but no statistical significance was found, nevertheless we can affirm that Pttg1 WT mice learned the task and consolidated better the learning than the Pttg1 KO mice.

3. Working memory errors

Working memory errors count the number of times that a mouse explores holes already explored. More working errors lead to longer session and worst search strategy. That is exactly what score plots are telling us in the RasGrf1 and RasGrf1-Pttg1: working error and total time variables are localized in the double positive quadrant, while spatial search strategy is in the double negative. In contrast, Pttg1 score plot is more diffuse because groups behave different between them.

There are no significant differences in Kruskal-Wallis in any period for any genotype, which means no group had more difficulties learning the task than the others. When we focus in the error bars, what we find is variability. It means that inside a group the performance quality is quite different.

Friedman's repeated measures test represents the improvement or impairment in the task performance. The results of this test were for RasGrf1 WT males ($\chi2(3)=0.03$, $p<0.05$) and KO ($\chi2(3)=0.026$, $p<0.05$) and for WT females ($\chi2(3)=0.005$, $p<0.05$; but no post hoc significance was found.

The four Pttg1 mice groups showed significant differences: WT males ($\chi2(3)=0.001$, $p<0.05$) and KO ($\chi2(3)=0.002$, $p<0.05$) and for WT female ($\chi2(3)=0.000$, $p<0.05$) and KO ($\chi2(3)=0.007$, $p<0.05$. With the post hoc test we observe a trend towards a difference for all groups from T1 to T2 but not in the rest, so the improvement took place during the learning period.

The RasGRf1-Pttg1 mice groups were also significant for this Friedman's test: WT males $\chi2(3)=0.000$, $p<0.05$; WT females $\chi2(3)=0.000$, $p<0.05$; KO males $\chi2(3)=0.001$, $p<0.05$; KO females $\chi2(3)=0.008$, $p<0.05$. In the post hoc test we observe two trends towards a difference: from T1 to T2 all groups improved and did less number of errors, but from MR to LR the impairment is evident, especially for male groups.

4. Spatial search strategy.

This is the most efficient search strategy. Analyzing the percentage of time that the mice spent using this search strategy and in which periods, we can obtain more detailed conclusions about this task learning. The less efficient strategy is random search, which was only used in T1 and some mice returned to it in RL. During T2 and MR mice preferred the serial search strategy preference because it was the easiest for them once they had learned that there was an escape hole.

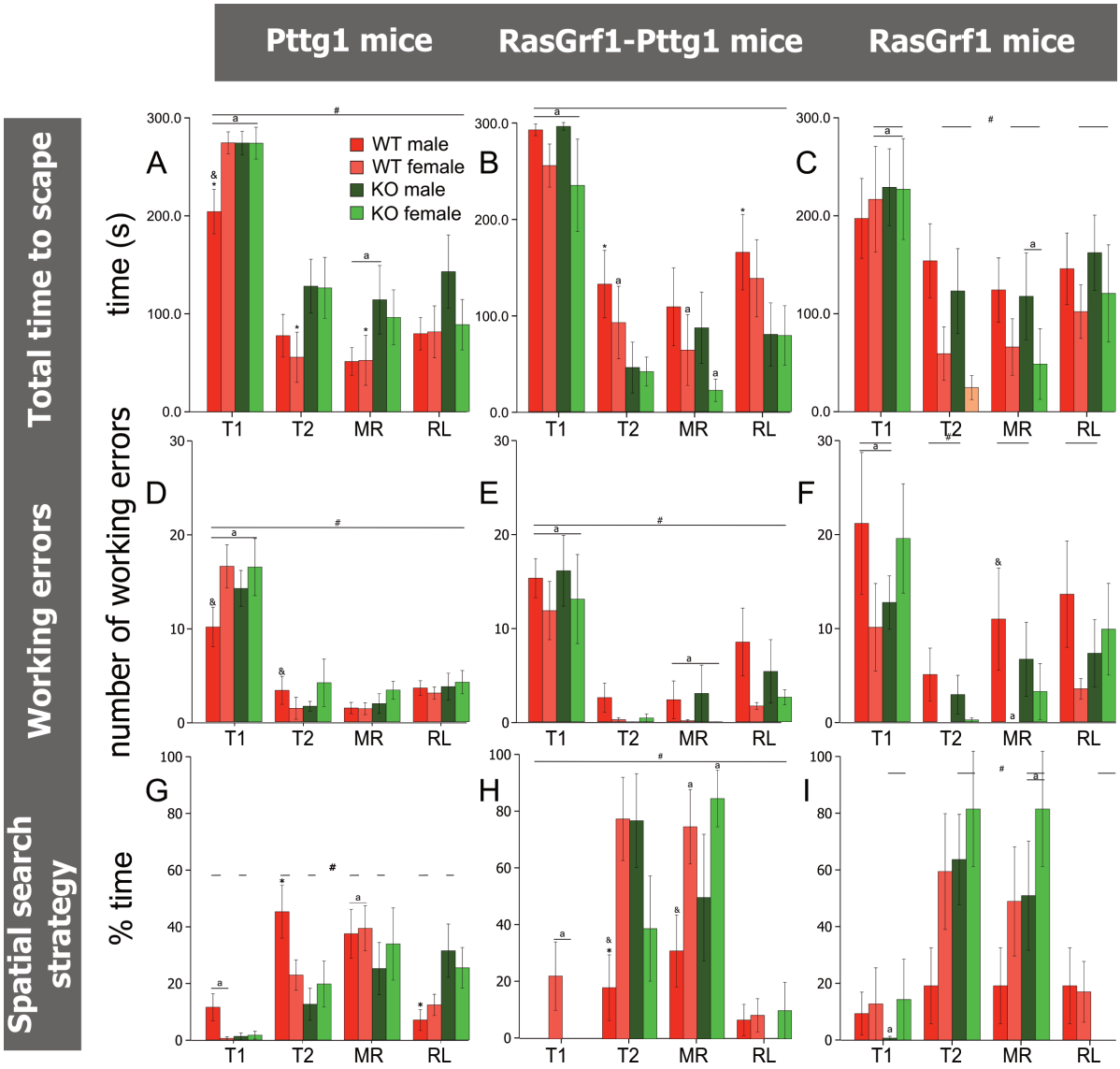

Fig 13. RasGrf1, Pttg1 and RasGrf1-Pttg1 WT and KO mice were tested once daily on the Barnes maze. Data represent performance of various maze indices, averaged for 4-day blocks during the first 4 days of training (T1); during the final 4 days of training (Days 19–22; T2); 12 days after the final day of training, when mice were retested for 4 days for memory retention (MR) of the spatial task; and immediately after memory retention tests, when mice received an additional 4 days of training on a memory reversal learning (RL) task where the escape hole location was reversed by 180°. Data represent group means plus or minus one standard error of the mean. Barnes maze # indicates a main effect, independent of genotype ($p<0.05$) ; a indicates a significant difference, independent of genotype, compared with the next period; * indicates a significant difference compared with KO mice of the same sex; & indicates a significant difference between mice of the same genotype and different sex.

RasGrf1 mice data show significant differences using the Friedman's test for KO groups: males $\chi2(3)=0.002$, $p<0.05$ and females $\chi2(3)=0.008$. For Pttg1 mice we have not found any signification between groups for the same period, but in T2 we got close: 0.055 $p>0.05$. Mann-Whitney test show us that WT and KO males were almost significant for that period: $U=23.5$, $r=-0.51$; 0.013 $p>0.0125$. WT males of this genotype were the only group to use this strategy more than the other three groups, especially in T2. This results support the idea that Pttg1 KO mice have impaired spatial learning abilities.

An interesting data from Pttg1 mice is the result obtained in RL period for this variable, when we have turned 180° the Barnes maze table. KO mice for both sexes use this strategy in similar percentage than in the previous period, MR. In contrast, both WT genders almost do not use it. The explanation is not that due their greater neuronal plasticity they have understood straight away that the escape hole changed its place, the objective of this period. The real explanation is, more likely, that they never learned exactly where it originally was and they started to search making no differences between maze's sides. This affirmation is based in the analysis of another results, the distance between the escape hole to the first hole explored (supplementary material). The only group that learned where the hole was during the training sessions was the WT male.

Double KO mice showed significant differences between periods to all the groups: WT males $\chi2(3)=0.029$, $p<0.05$; WT females $\chi2(3)=0.002$, $p<0.05$; KO males $\chi2(3)=0.007$, $p<0.05$; KO females $\chi2(3)=0.016$, $p<0.05$. Even if there is only the WT female group significant for the post hoc analysis from MR to RL, there are trends towards a difference for KO females at the same period and from T1 to T2 for WT females and KO males. Between groups we just find signification for the T2: $H(3)=9,024$, $p<0.05$, but in the post hoc none of them were statistically significant.

It is known that NR2A and NR2B subunits insulin-dependent phosphorylation modulates NMDA activation [179]. Two years ago, a relation between insulin and spatial learning was described [180]. Starved Pttg1 KO male mice at 3 months of age have reduced insulin levels in a 50% [79]. This difference between KO males and females, who show an increased insulin sensibility, could be a reason for the total separation in a PCA score plot when we compare only the WT and KO male groups. In contrast, we do find WT and KO females mixed on the score plot when we use this comparative test (data not shown). However, the statistical test did not show any significant differences neither important trend towards a difference between male and female KO groups, so we do not think that is the reason for their impaired spatial behavior, but more likely WT males over performed during the task so differences between WT and KO females were not as big as between WT and KO males.

RasGrf1-Pttg1 KO mice behaved in a similar way than RasGrf1 KO females: females from both genotypes learned better how to resolve the task, especially RasGrf1 ones, and in both, in general, KO groups learned to resolve it equal to or better than the WTs. RasGrf1 KO genotype predominance in RasGRf1-Pttg1 KO mice in the phenotype showed by the hippocampus spatial function must keep some relation with the function of these proteins function in this organ's development or synaptic plasticity. We think that a plausible reason is that transcriptoma changes dues to Rasgrf1 deletion dominate over the changes dues to Pttg1 deletion.

In conclusion, Pttg1 KO mice show an impaired spatial behavior, so they must have one or more hippocampal functions affected. Pttg1 deletion could be causing developmental problems in this organ. Another hypothesis is that one or more of its non-canonical functions is affected due to its absence and this could cause synaptic plasticity defects and led to an impaired spatial memory.

III. Role of RasGrf1 and Pttg1 in body weight and glucose homeostasis

In order to complete the most interesting aspects for us about the phenotypic characterization of RasGrf1$^{-/-}$-Pttg1$^{-/-}$ mice, we decided to measure their weight gain and analyze their glucose homeostasis.

1. Evolution of mice gain weight

A reduced body mass has been described for males in most RasGrf1 KO mice lines [68, 76-78] as well as a weight increase in the transgenic mice line where RasGrf1 is overexpressed [74]. These data confirm the important role that RasGrf1 plays in postnatal body development [178]. Meanwhile, Pttg1 KO mice show a reduced weight compared to their controls at 5 months of age, although female mice do not show this phenotype [79]. An interesting data is that RasGRf1 KO mice display a reduced levels of IGF-1 (insulin growth factor) [68, 76, 78] and Pttg1 expression in breast cancer cells and malign astrocytes is IGF-1/PI3K/Akt dependent [181, 182]. IGF-1 signaling pathway contributes to growth during puberty [183] as well as to the growth of pancreatic β cells, as it has been described that in mice showing IGF-1 upregulation, a specific hyperplasia of these cells is observed [184].

a. Non-weaned pups

During the first 23 days of life, pups live in the same cage as their parents, until they are weaned. We weighted 23 animals from each group but not every day all of them.

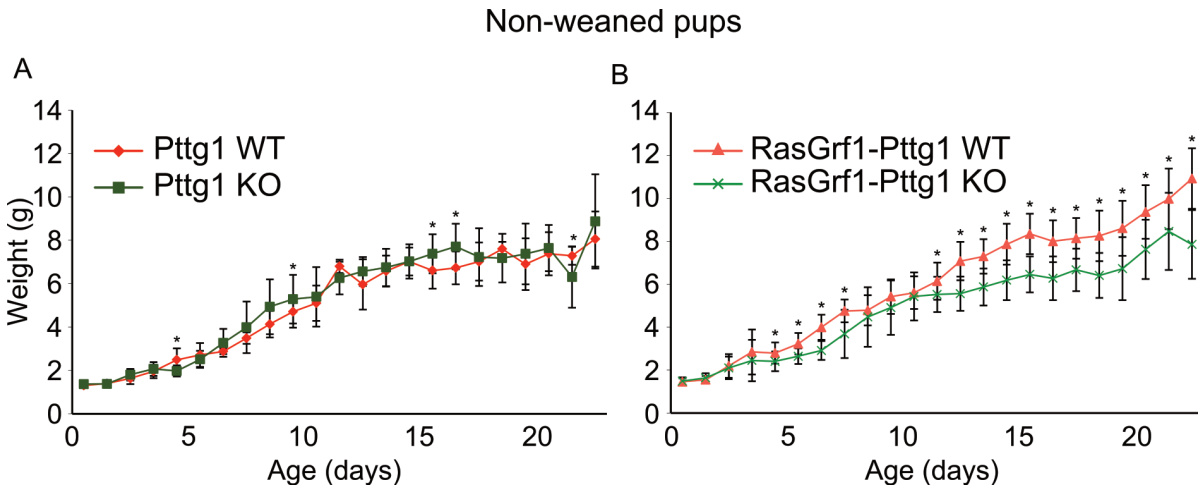

Fig 14. Representative graph of the weight means during weaning. **A.** Pttg1 pups data. **B.** RasGrf1-Pttg1 mice data. Error bars represent ±DE. *, p<0.05 (t-test).

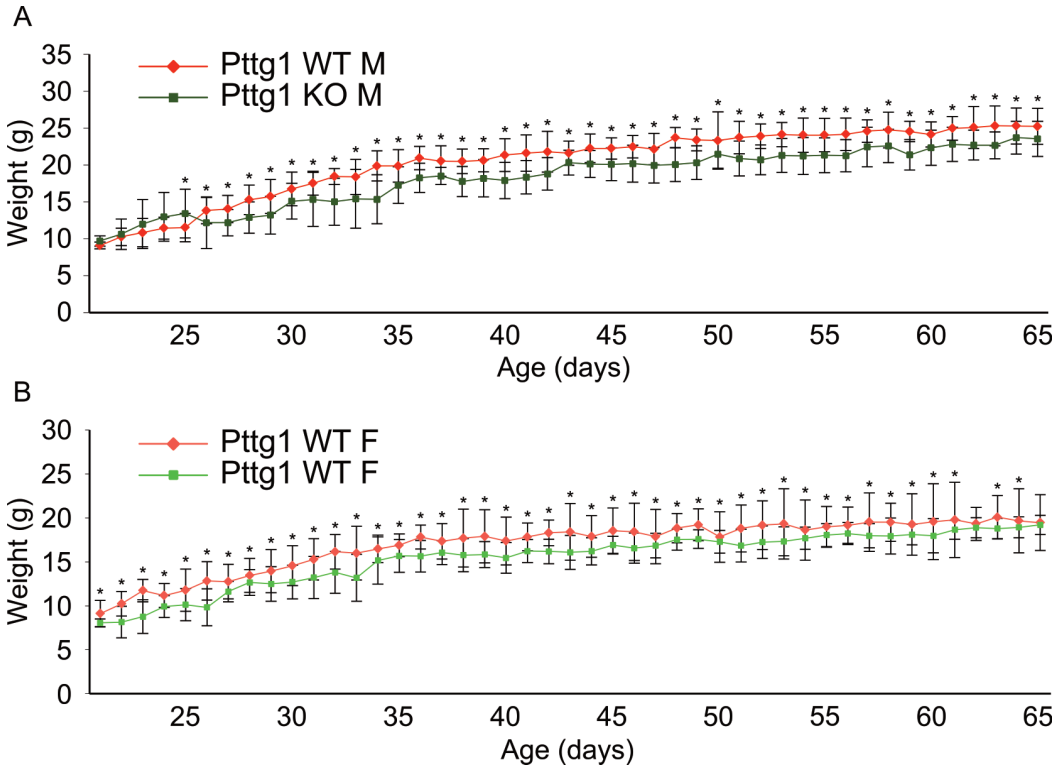

Fig 15. WT and KO Pttg1 mice from 23 to 65 days of age. **A.** WT and KO male Pttg1 mice data. **B.** Data from WT and KO female Pttg1 animals. *, p<0.05 (t-test). Errors bars represent ±DE.

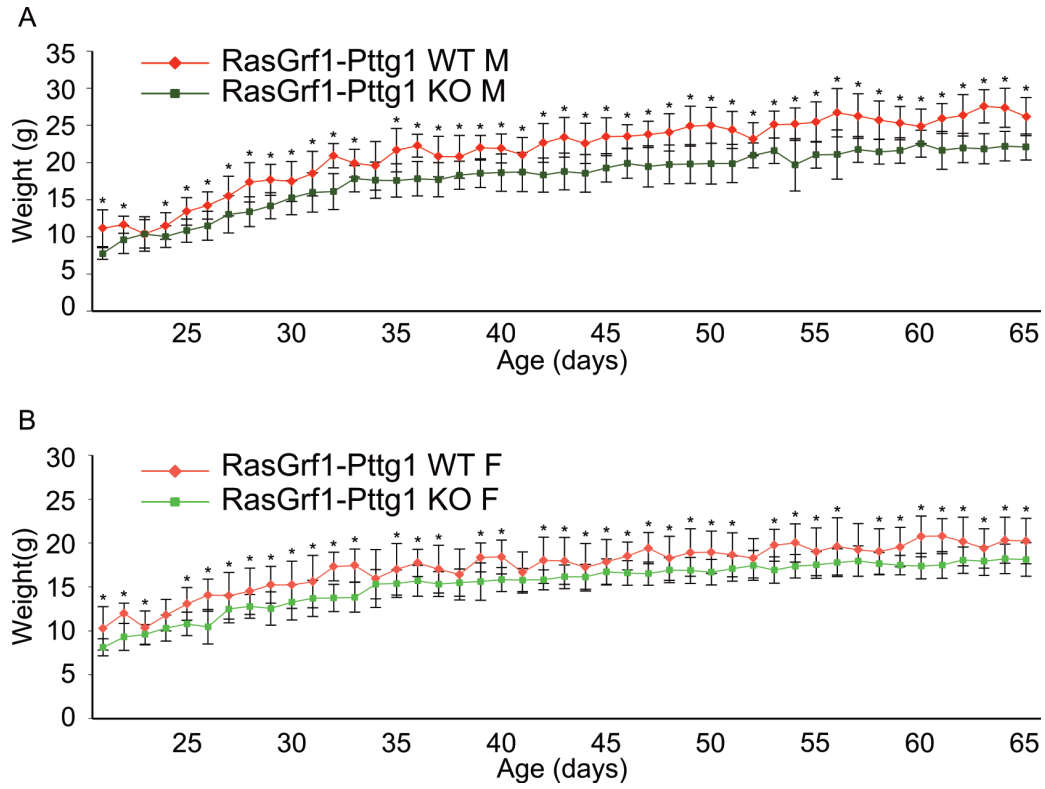

Fig 16. Post-weaning weight of WT and KO RasGrf1-Pttg1 mice. **A.** WT and KO RasGrf1-Pttg1 males. **B.** Data from WT and KO females. *, p<0.05 (t-test). Errors bars represent ±DE.

Pttg1 KO mice did not show differences compared to their controls. We then compared RasGrf1-Pttg1 WT and Pttg1 WT groups and statistical differences arose (data not shown), even if we had carefully homogenized their genetic background. We suppose that bad coincidence when choosing litters or particular circumstances could be responsible for this unexpected result.

RasGrf1-Pttg1 mice show significant differences ($p<0.05$) between WT and KO groups, especially from the 13th day, where we appreciate how WT group starts gaining weight in a sustained manner while the increase in the body mass gain of KO mice is slower. Pttg1 KO and RasGrf1-Pttg1 KO groups do not show differences, so we can conclude that RasGrf1-Pttg1 KO non-weaned pups show the same reduced body mass phenotype as Pttg1 KOs.

b. Weaned pups

.- From 23 to 65 days of age.

Significant differences are found between Pttg1 WT and KO male mice (Fig.A) from the 25th day of age. WT mice gain weight faster that KO from 26 to 36 day, but then the rhythm slows down. In contrast, KO male mice gain weight in a sustained manner. Comparing with the published results for two months of age [79], we observe that there are no differences between our data and the published results. Signification in our case is due to the big number of mice used, so we can distinguish a subtle but constant difference of weight.

Female Pttg1 weaned KO mice also show a diminished body weight comparing to WT female mice. At the end of this period, between 62 and 65 days, differences become smaller pointing to a similar adult body weight.

Differences between males in RasGrf1-Pttg1 KO and WT groups increase through time, especially from 42 and on. Double KO female mice keep a small but significant difference between both groups during all the experiment. Comparing to the previous data from the Pttg1 mice data, we can confirm a slight aggravation of body mass reduction for female and male RasGrf1-Pttg1 KO pups during the first month of life compared to the female and male Pttg1 KO pups.

.- • Three months of age

RasGrf1-Pttg1 mice at three months of age show significant differences in their body weight depending on their genotype and sex $F(3, 38.041)=38.311$, $p<0.001$, $\omega=0.57$. Bonferroni post hoc test shows significant differences between WT males and the three other

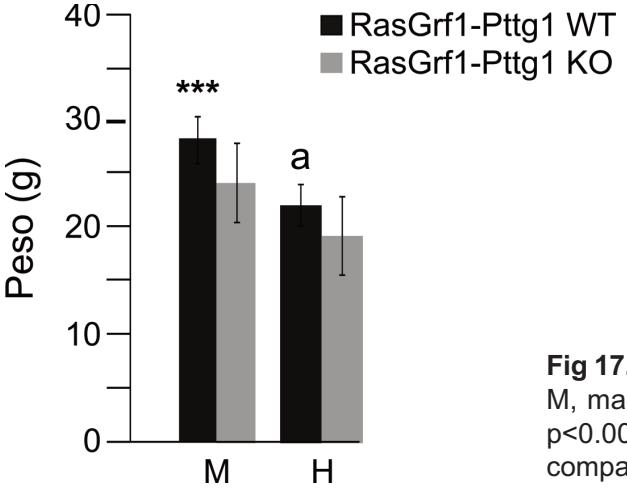

groups, but also that WT and KO female groups are statistically different. We do not observe differences when comparing with published data regarding male RasGrf1 [78] or Pttg1 [79] data.

Fig 17. Weight of 3 months old RasGrf1-Pttg1 mice. M, male. F, female. Error bars represent ±DE. ***, p<0.001, comparing to the rest of groups. a, p<0.05 compared to the other group of the same sex.

.- Ten months of age

Independent one-way ANOVA test for Pttg1 ten months-old mice data show significant differences $F(3, 15)=13.210$, $p<0.001$, $\omega=0.81$. Bonferroni post hoc test shows that WT males are heavier than females or KO males. Our RasGrf1 mice line has lost its reduced body weight phenotype at ten months of age. Regarding RasGRf1-Pttg1 10 months-old mice, an effect of sex and genotype is observed, $F(3, 31)=21.254$, $p<0.001$, $\omega=0.8$. As shown for the 3 months-old mice, on the Pttg1 analysis at 10 months Bonferroni test finds significant differences between WT males and the rest, but also between both female groups.

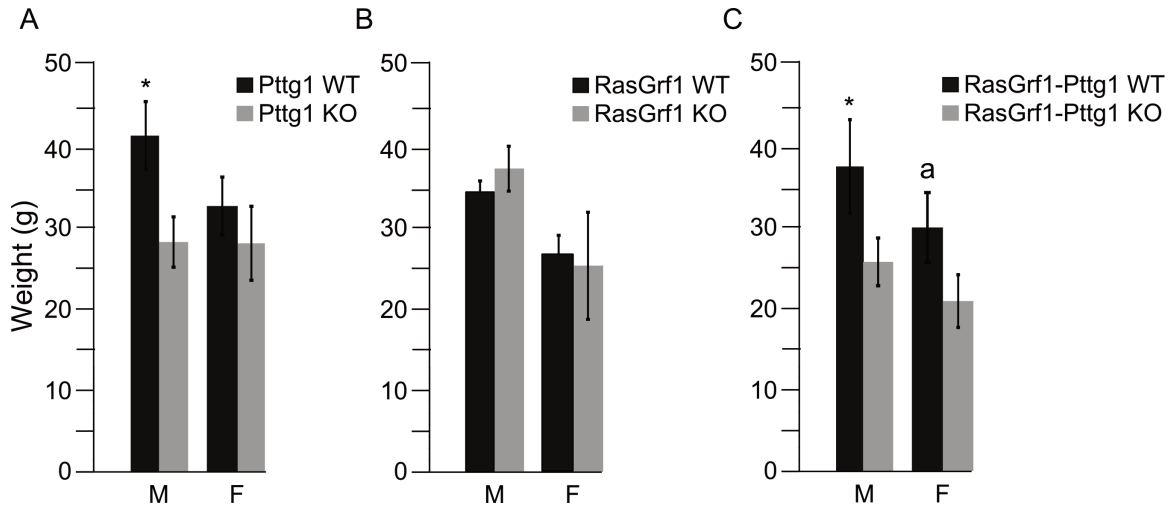

Fig 18. Weight for the three genotypes at 10 months of age. **A.** Graph obtained using Pttg1 mice data. **B.** Data from RasGrf1 mice. **C.** Weight of RasGrf1-Pttg1 mice. M, males. F, females. Error bars represent ±DE of the mean. *, p<0.05, comparing with the rest of groups. a, p<0.05 compared to the other group of the same sex.

Differences between WT and KO male Pttg1 mice at 10 months of age have already been published [79], but in our results, KO mean is 5 g lower than in Wang et al. work. Double KO mice from both sexes show a reduced body weight, even with the loss of phenotype of the RasGrf1 mice used for their generation. It very interesting the reduction of weight in the double KO females compared with the Pttg1 KO ones.

2. Glucose tolerance test (GTT)

Another goal for this study was the analysis of glucose-stimulated insulin secretion in RasGrf1-Pttg1 mice. First, we studied this parameter at three months of age to compare the data with the published studies for RasGrf1 [78] and Pttg1 [79] mice. In addition, we wanted to study the evolution of the phenotype and check their insulin secretion at ten months of age, so we would be able to compare these results with ten months-old Pttg1 and RasGrf1 simple KO mice [79].

a. GTT in three months old RasGrf1-Pttg1 mice

.- Insulin levels

No genotype or sex effect was found in insulin levels for RasGrf1-Pttg1 mice with independent one-way ANOVA test. (Fig. 19 A). When comparing WT and KO males data applying t-test we obtained the next significances:

- t=0: WT (M=1,06, SE=0,36); double KO (M=0,17, SE=0,06) $p<0,05$
- t=30: WT (M=0,52, SE=0,09); double KO (M=0,26, SE=0,06) $p<0,05$
- t=90: WT (M=0,44, SE=0,08); double KO (M=0,22, SE=0,05) $p<0,05$

The same comparison with female data did not show any significance. We obtained similar results to those published for male mice at three months of age [79]. RasGrf1 KO data published by Font de Mora et al. [78] also show a statistical difference at 0' point, but RasGrf1-Pttg1 display an aggravated phenotype compared with RasGrf1 KO mice. Double KO females display a phenotype similar to Pttg1 simple KOs, but as there are no published data regarding RasGrf1 KO females, no comparison is possible.

.- Glucose levels

Independent one-way ANOVA found significant differences at t 30' $F(3, 33)=5.224$, $p<0.01$, $\omega= 0.51$ and t 90' $F(3, 33)=7.602$ $p<0.01$, $\omega=0.59$. No signification was found with post hoc tests. This parameter is significantly aggravated when comparing to data from Pttg1 KO and RasGrf1 KO mice data at the same age. Blood glucose values displayed by RasGrf1 WT and KO mice in the study by Font de Mora et al. are not so high and they do not in-

crease between 15 to 30 and 30 to 90 minutes [78]. Pttg1 KO male group at this age do not show differences with their control group [79]. Double KO females behaved as we expected, showing no differences with the control groups.

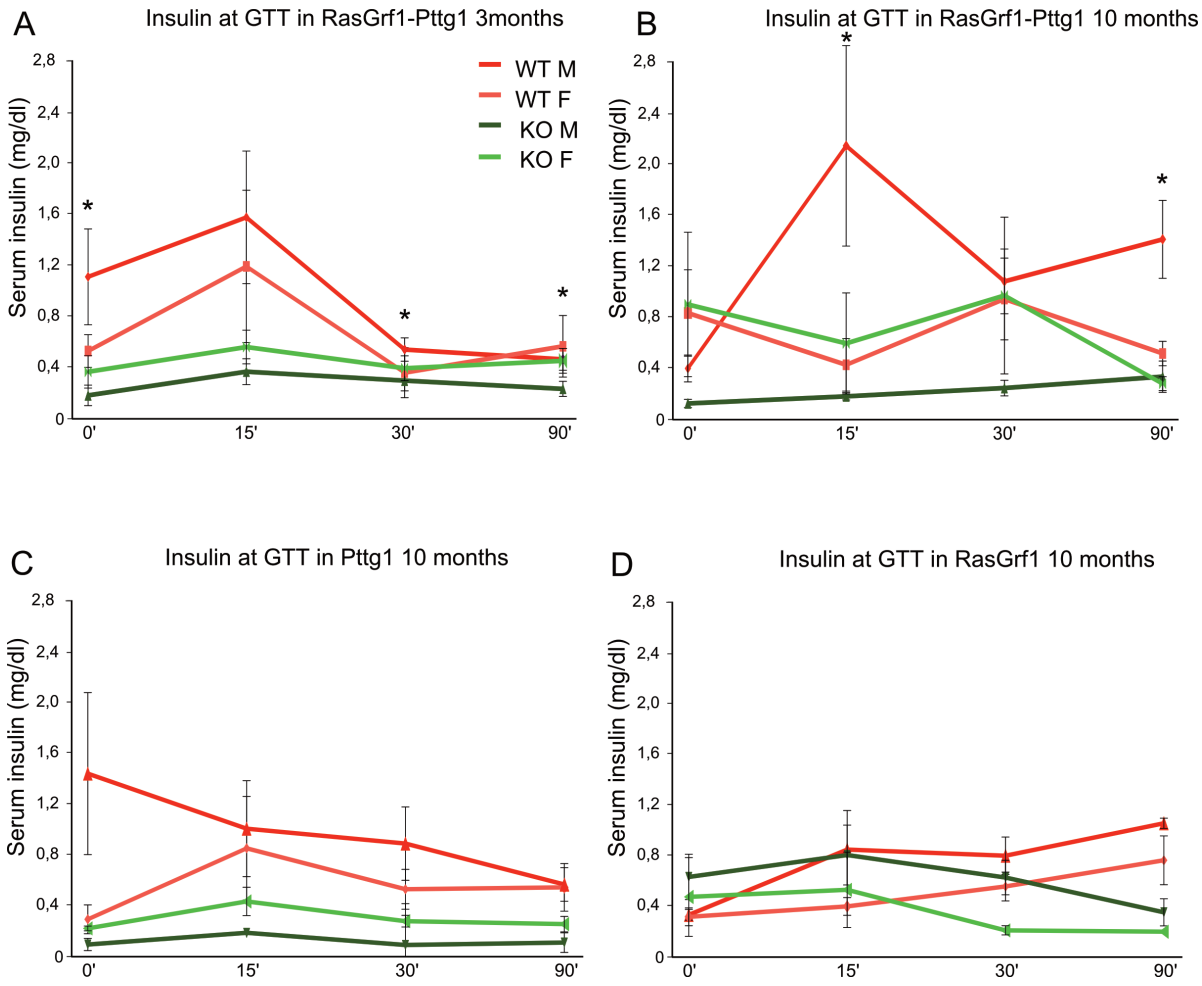

Fig 19. Insulin levels obtained during GTT. **A.** RasGrf1-Pttg1 mice data at 3 months of age. **B.** RasGrf1-Pttg1 mice data at 10 months of age. **C.** RasGrf1 mice data at 10 months of age. **D.** Pttg1 mice data at 10 months of age. Errors bars represent ±DE. *, p<0.05, comparing with the rest of groups.

b. GTT in ten month-old animals

.- Insulin levels

- RasGrf1-Pttg1 mice:

An effect depending on sex and genotype effect is obtained with ANOVA test at 15' $F(3, 30)= 4{,}725$, $p<0.01$, $\omega= 0.5$ and at 90' $F(3, 22)= 9.709$, $p<0.001$, $\omega= 0.7$.

Gabriel post hoc test, for slightly different sample sizes, shows that at these two time points WT males are significantly different.

- RasGrf1 mice:

We find a significant effect depending on genotype and sex in mice insulin levels at 30' $F(3, 20)= 3.292$, $p<0.05$, $\omega= 0.46$.

- Pttg1 mice:

We do not find any statistical differences for this genotype, but we do observe a trend towards a difference that, upon an increase in sample size, could be significant.

In the results of the insulin levels from ten month-old mice (Fig. 19 B, C, D), first thing drawing our attention are differences between WT mice. Fig. B WT males, with a great error, shows even higher insulin levels than at 3 months of age, something weird when it is known the number of islets reduction with age, and so the insulin release. The high sensibility of the insulin detection kit might be responsible of these measurement errors. We will consider RasGrf1 WT mice data for discussion as they should be more reliable because of their low error rate and their similarity to Pttg1 WT mice.

Regarding the KO mice, the only genotype in which males produce insulin levels above the females is the RasGrf1 KO. At 15' and 30' their serum insulin levels are similar to the WT males, but at 90' their levels decay, while in the WT male group a slight increases is observed. This data show that RasGrf1 KO mice, both males and females, are able to release the same amount of insulin than the WTs, but the level start decaying earlier.

Ten months-old Pttg1 KO male mice barely release 0.2 ng/ml insulin when stimulated, but females release approximately the double of that amount. Insulin levels of Pttg1 KO mice are really changed. RasGrf1-Pttg1 KO male mice show a phenotype similar to Pttg1 KO male, but RasGrf1-Pttg1 KO females are more similar to WT females. We conclude that RasGrf1- Pttg1 KO male mice show a seriously impaired age-independent insulin release, as Pttg1 and RasGrf1 simple KO phenotype for this parameter.

To sum up, RasGrf1 absence in male and female mice at 10 months of age does not produce a reduction in the insulin released amount at the first time points of the GTT, but they are not able to reach WT levels at 90'. RasGrf1-Pttg1 and Pttg1 KO male groups at ten months of age are not able to increases their insulin levels when a glucose stimulus is applied, while females respond in a first moment releasing an amount similar to the WT females, but at 90' insulin decays to KO males levels.

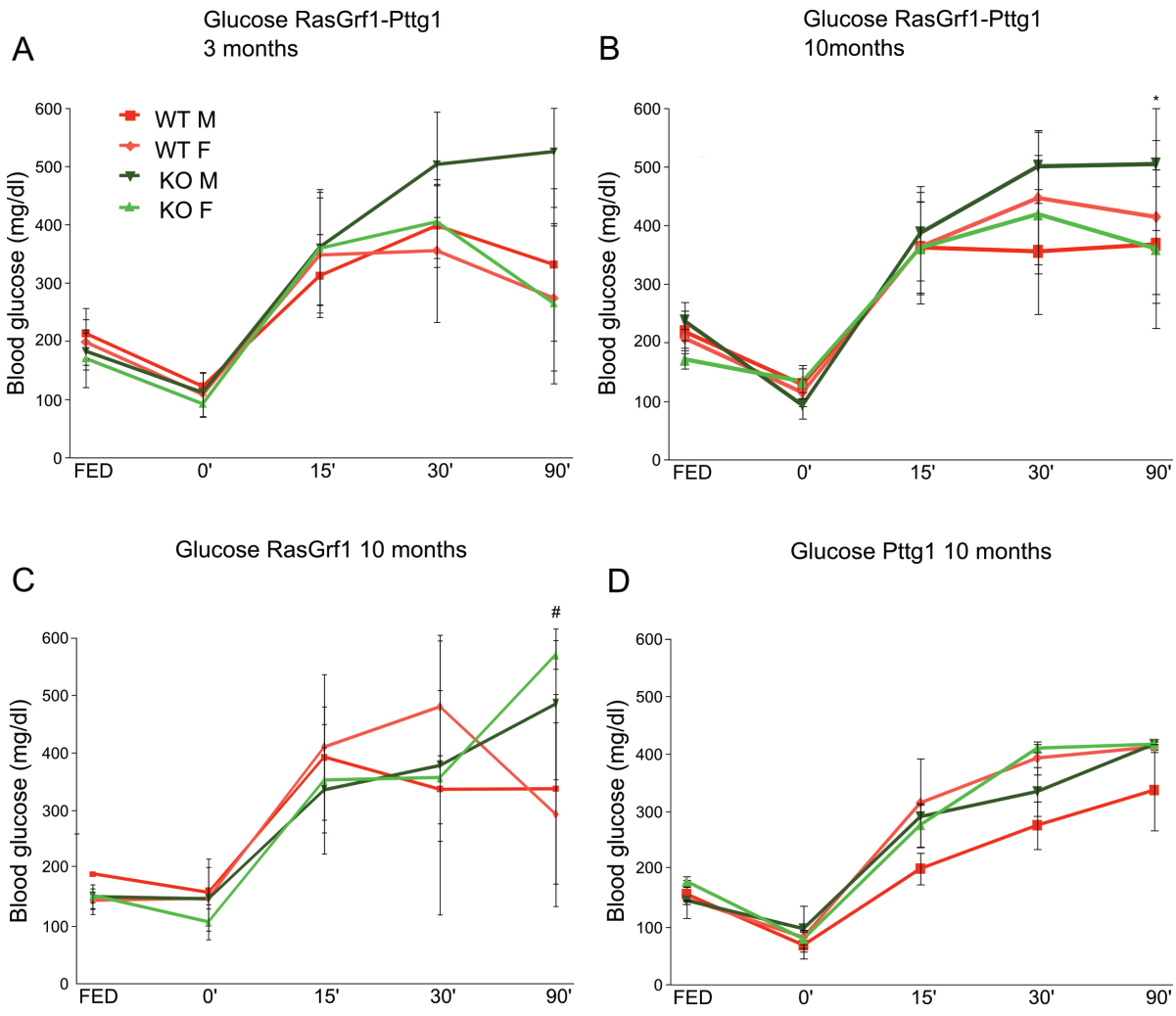

Fig 26. Gráficas representativas de las medias de los niveles de glucosa obtenidos durante la prueba de tolerancia a la glucosa. **A.** Datos de los ratones RasGrf1-Pttg1 a los 3 meses. **B.** Datos de los ratones RasGrf1-Pttg1 a los 10 meses. **C.** Datos de los ratones RasGrf1 a los 10 meses. **D.** Datos de los ratones Pttg1 a los 10 meses. Las barras de error representan ±DE. *, p<0,05, entre machos. #, p<0,05 entre hembras.

.- Blood glucose levels

- RasGrf1-Pttg1 mice:

ANOVA statistical test shows a significant effect depending on sex and genotype in the analysis of blood glucose levels in mice at the basal state $F(3, 27)=9.761$, $p<0.001$, $\omega= 0.67$; at t 0' $F(3, 31)=5.481$, $p<0.01$, $\omega= 0.52$ y at t 30' $F(3, 31)=3.584$, $p<0.05$, $\omega= 0.42$.

Bonferroni and Gabriel post hoc tests confirmed that data from RasGrf1-Pttg1 KO females is statistically different to glucose found in double KO and WT male groups. At 90' there exist significant differences between both male groups.

- RasGrf1 mice:

At 90’ we find a significant effect that depends on both sex and genotype $F(3, 16)=3.900$, $p<0.05$, $\omega=0.55$. With Gabriel post hoc test we see significant differences between both female groups.

- Pttg1 mice:

An effect depending on genotype and sex is found at the basal state $F(3, 5.59)=15.422$, $p<0.01$, $\omega= 0.43$; at 15’ $F(3, 13)=5.263$, $p<0.05$, $\omega= 0.65$; at 30’ $F(3, 4.866)=15.733$, $p< 0.01$, $\omega= 0.86$ y at 90’ $F(3, 12)=4.234$, $p<0.05$, $\omega=0.61$.

Appling Bonferroni and Gabriel post hoc tests, we do not find any significant difference at basal state or at 90’. At 15’ WT male group is significantly different that WT females and there is a trend towards a difference with KO groups. At the 30’ time point WT male group is statistically different than both females groups, meanwhile the KO male group is significantly different than the KO females.

Glucose catabolism aggravates with age, as we can see comparing Fig. A and Fig. B., but we are only able to find significant changes at 90’ in RasGrf1-Pttg1 male Kos. Double KO males do not aggravate their insulin rate with age, as shown into Fig 20 A and B. At ten months, the three female groups display higher glucose peaks than control males, pointing to sex-dependent glycemic metabolism impairment related to age in mice.

Results for RasGrf1 and Pttg1 KO mice results at 10 months of age are still more exciting. Male and female RasGrf1 deficient mice, in spite their higher insulin levels in GTT were higher than Pttg1 KO ones, were not able to decrease their blood glucose levels. If we analyze in detail, the evolution of the glucose curve of RasGrf1 KO mice matches well with the insulin one. During the first half hour after glucose injection, insulin and glucose levels in controls and KO are similar, but at 90’, insulin levels decay and, in consequence, blood glucose goes up. We would like to draw your attention on the RasGrf1 KO female group, whose performance was totally unexpected. As Wang explains, estrogen increases tissues insulin sensibility and that is the reason behind the Pttg1 KO females GTT performance [79], but maybe at ten months of age estrogen is not enough. Pttg1 KO mice and WT females show the highest value of the glucometer used, 600 mg/dl.

In conclusion, we confirm a similar Pttg1 KO mice phenotype compared to the RasGrf1 KO and double KO mice on insulin β cell release and glucose homeostasis. RasGrf1 and Pttg1 are involved in Langerhans islets maintenance and release and, in consequence, glucose catabolism.

Conclusions

1. Stable clones of Pttg1 silenced PC12 cells show an increased proliferation rate while the RasGrf1 silenced PC12 clones display a reduction of this rate. Furthermore, stable overexpression of RasGrf1 in this cell line increases their proliferation rate.

2. Stable downregulation of RasGrf1 and Pttg1 in PC12 cells causes chromosomal instability.

3. PC12 cells with stable RasGrf1 knock down show an influence in short-term ERK1/2 phosphorylation, meanwhile activated Akt, JNK and p38 present no changes.

4. Pttg1 promoter activity is partially regulated by the ERK signaling pathway. In BTC3 and PC12 cell lines, where RasGrf1 is naturally expressed, the activity of this promoter is affected in a different way than in COS1 and 293T cell lines, where it is not. Moreover, RasGrf1 overexpression in BTC3 cell line positively influences the Pttg1 promoter activity. In PC12 cells, to observe this stimulation, in addition to RasGrf1 overexpression, NGF induction is required.

5. Pttg1 KO mice show impaired spatial learning and memory. The RasGrf1 KO lineage generated in our laboratory does not display this impairment. RasGrf1-Pttg1 double KO mice, like RasGrf1 KO mice, show no phenotype.

6. RasGrf1-Pttg1 KO mice of all ages exhibit a reduced body weight. Male and female mice double KO mice at 10 months of age show a lower body weight than Pttg1 KO animals at the same age.

7. Three months-old double KO male mice display the same glucose homeostasis phenotype during the glucose tolerance test than the Pttg1 KO male mice, which is aggravated compared to the RasGrf1 KO male mice at the same age. Female double KO animals at that age show the same phenotype than Pttg1 KO female mice.

8. Ten months-old RasGrf1-Pttg1 double KO mice present a similar phenotype during the glucose tolerance test than three months-old animals. At ten months of age, the three genotypes exhibit similar glucose homeostasis phenotypes during this test.

References

1. Fernandez-Medarde, A. and E. Santos, *The RasGrf family of mammalian guanine nucleotide exchange factors.* Biochim Biophys Acta, 2011. **1815**(2): p. 170-88.
2. Wolfman, A. and I.G. Macara, *A cytosolic protein catalyzes the release of GDP from p21ras.* Science, 1990. **248**(4951): p. 67-9.
3. Martegani, E., et al., *Cloning by functional complementation of a mouse cDNA encoding a homologue of CDC25, a Saccharomyces cerevisiae RAS activator.* EMBO J, 1992. **11**(6): p. 2151-7.
4. Gotoh, T., et al., *Activation of R-Ras by Ras-guanine nucleotide-releasing factor.* J Biol Chem, 1997. **272**(30): p. 18602-7.
5. Innocenti, M., et al., *CDC25(Mm)/Ras-GRF1 regulates both Ras and Rac signaling pathways.* FEBS Lett, 1999. **460**(2): p. 357-62.
6. Quilliam, L.A., et al., *M-Ras/R-Ras3, a transforming ras protein regulated by Sos1, GRF1, and p120 Ras GTPase-activating protein, interacts with the putative Ras effector AF6.* J Biol Chem, 1999. **274**(34): p. 23850-7.
7. Wei, W., et al., *Localization of the cellular expression pattern of cdc25NEF and ras in the juvenile rat brain.* Brain Res Mol Brain Res, 1993. **19**(4): p. 339-44.
8. Zippel, R., et al., *Ras-GRF, the activator of Ras, is expressed preferentially in mature neurons of the central nervous system.* Brain Res Mol Brain Res, 1997. **48**(1): p. 140-4.
9. Guerrero, C., et al., *Expression of alternative forms of Ras exchange factors GRF and SOS1 in different human tissues and cell lines.* Oncogene, 1996. **12**(5): p. 1097-107.
10. Cullen, P.J. and P.J. Lockyer, *Integration of calcium and Ras signalling.* Nat Rev Mol Cell Biol, 2002. **3**(5): p. 339-48.
11. Farnsworth, C.L., et al., *Calcium activation of Ras mediated by neuronal exchange factor Ras-GRF.* Nature, 1995. **376**(6540): p. 524-7.
12. Buchsbaum, R., et al., *The N-terminal pleckstrin, coiled-coil, and IQ domains of the exchange factor Ras-GRF act cooperatively to facilitate activation by calcium.* Mol Cell Biol, 1996. **16**(9): p. 4888-96.
13. Freshney, N.W., S.D. Goonesekera, and L.A. Feig, *Activation of the exchange factor Ras-GRF by calcium requires an intact Dbl homology domain.* FEBS Lett, 1997. **407**(1): p. 111-5.
14. Arozarena, I., et al., *Activation of H-Ras in the endoplasmic reticulum by the RasGRF family guanine nucleotide exchange factors.* Mol Cell Biol, 2004. **24**(4): p. 1516-30.
15. Krapivinsky, G., et al., *The NMDA receptor is coupled to the ERK pathway by a direct interaction between NR2B and RasGRF1.* Neuron, 2003. **40**(4): p. 775-84.
16. Schmitt, J.M., et al., *Calmodulin-dependent kinase kinase/calmodulin kinase I activity gates extracellular-regulated kinase-dependent long-term potentiation.* J Neurosci, 2005. **25**(5): p. 1281-90.

17. Li, S., et al., *Distinct roles for Ras-guanine nucleotide-releasing factor 1 (Ras-GRF1) and Ras-GRF2 in the induction of long-term potentiation and long-term depression.* J Neurosci, 2006. **26**(6): p. 1721-9.
18. Jin, S.X. and L.A. Feig, *Long-term potentiation in the CA1 hippocampus induced by NR2A subunit-containing NMDA glutamate receptors is mediated by Ras-GRF2/Erk map kinase signaling.* PLoS One, 2010. **5**(7): p. e11732.
19. Gu, F., et al., *Translational responses of NR2B overexpression in the cerebral cortex of transgenic mice: a liquid chromatography-based proteomic approach.* Brain Res, 2009. **1250**: p. 1-13.
20. Buchsbaum, R.J., B.A. Connolly, and L.A. Feig, *Interaction of Rac exchange factors Tiam1 and Ras-GRF1 with a scaffold for the p38 mitogen-activated protein kinase cascade.* Mol Cell Biol, 2002. **22**(12): p. 4073-85.
21. Buchsbaum, R.J., B.A. Connolly, and L.A. Feig, *Regulation of p70 S6 kinase by complex formation between the Rac guanine nucleotide exchange factor (Rac-GEF) Tiam1 and the scaffold spinophilin.* J Biol Chem, 2003. **278**(21): p. 18833-41.
22. Tian, X. and L.A. Feig, *Age-dependent participation of Ras-GRF proteins in coupling calcium-permeable AMPA glutamate receptors to Ras/Erk signaling in cortical neurons.* J Biol Chem, 2006. **281**(11): p. 7578-82.
23. Norum, J.H., et al., *Endogenous expression and protein kinase A-dependent phosphorylation of the guanine nucleotide exchange factor Ras-GRF1 in human embryonic kidney 293 cells.* FEBS J, 2005. **272**(9): p. 2304-16.
24. Kesavapany, S., et al., *Neuronal nuclear organization is controlled by cyclin-dependent kinase 5 phosphorylation of Ras Guanine nucleotide releasing factor-1.* Neurosignals, 2006. **15**(4): p. 157-73.
25. Bhattacharya, M., A.V. Babwah, and S.S. Ferguson, *Small GTP-binding protein-coupled receptors.* Biochem Soc Trans, 2004. **32**(Pt 6): p. 1040-4.
26. Ritter, S.L. and R.A. Hall, *Fine-tuning of GPCR activity by receptor-interacting proteins.* Nat Rev Mol Cell Biol, 2009. **10**(12): p. 819-30.
27. Inglese, J., et al., *G beta gamma interactions with PH domains and Ras-MAPK signaling pathways.* Trends Biochem Sci, 1995. **20**(4): p. 151-6.
28. Shou, C., et al., *Differential response of the Ras exchange factor, Ras-GRF to tyrosine kinase and G protein mediated signals.* Oncogene, 1995. **10**(10): p. 1887-93.
29. Zippel, R., et al., *The brain specific Ras exchange factor CDC25 Mm: modulation of its activity through Gi-protein-mediated signals.* Oncogene, 1996. **12**(12): p. 2697-703.
30. Mattingly, R.R. and I.G. Macara, *Phosphorylation-dependent activation of the Ras-GRF/CDC25Mm exchange factor by muscarinic receptors and G-protein beta gamma subunits.* Nature, 1996. **382**(6588): p. 268-72.
31. Mattingly, R.R., V. Saini, and I.G. Macara, *Activation of the Ras-GRF/CDC25Mm exchange factor by lysophosphatidic acid.* Cell Signal, 1999. **11**(8): p. 603-10.
32. Yang, H., et al., *Phosphorylation of the Ras-GRF1 exchange factor at Ser916/898 reveals activation of Ras signaling in the cerebral cortex.* J Biol Chem, 2003. **278**(15): p. 13278-85.
33. Norum, J.H., et al., *Epac- and Rap- independent ERK1/2 phosphorylation induced by Gs-coupled receptor stimulation in HEK293 cells.* FEBS Lett, 2007. **581**(1): p. 15-20.
34. Kiyono, M., T. Satoh, and Y. Kaziro, *G protein beta gamma subunit-dependent Rac-guanine nucleotide exchange activity of Ras-GRF1/CDC25(Mm).* Proc Natl Acad Sci U S A, 1999. **96**(9): p. 4826-31.
35. Robinson, K.N., et al., *Neurotrophin-dependent tyrosine phosphorylation of Ras guanine-releasing factor 1 and associated neurite outgrowth is dependent on the HIKE domain of TrkA.* J Biol Chem, 2005. **280**(1): p. 225-35.
36. Yang, H. and R.R. Mattingly, *The Ras-GRF1 exchange factor coordinates activation of H-Ras and Rac1 to control neuronal morphology.* Mol Biol Cell, 2006. **17**(5): p. 2177-89.

37. Talebian, A., et al., *Ras Guanine Nucleotide Releasing Factor 1 (RasGrf1) Enhancement of Trk Receptor-Mediated Neurite Outgrowth Requires Activation of Both H-Ras and Rac.* J Mol Neurosci, 2012.
38. Kiyono, M., Y. Kaziro, and T. Satoh, *Induction of rac-guanine nucleotide exchange activity of Ras-GRF1/CDC25(Mm) following phosphorylation by the nonreceptor tyrosine kinase Src.* J Biol Chem, 2000. **275**(8): p. 5441-6.
39. Giglione, C., S. Gonfloni, and A. Parmeggiani, *Differential actions of p60c-Src and Lck kinases on the Ras regulators p120-GAP and GDP/GTP exchange factor CDC25Mm.* Eur J Biochem, 2001. **268**(11): p. 3275-83.
40. Kiyono, M., et al., *Stimulation of Ras guanine nucleotide exchange activity of Ras-GRF1/CDC25(Mm) upon tyrosine phosphorylation by the Cdc42-regulated kinase ACK1.* J Biol Chem, 2000. **275**(38): p. 29788-93.
41. Arozarena, I., et al., *The Rho family GTPase Cdc42 regulates the activation of Ras/MAP kinase by the exchange factor Ras-GRF.* J Biol Chem, 2000. **275**(34): p. 26441-8.
42. Arozarena, I., D. Matallanas, and P. Crespo, *Maintenance of CDC42 GDP-bound state by Rho-GDI inhibits MAP kinase activation by the exchange factor Ras-GRF. evidence for Ras-GRF function being inhibited by Cdc42-GDP but unaffected by CDC42-GTP.* J Biol Chem, 2001. **276**(24): p. 21878-84.
43. Rabiet, M.J., et al., *Inhibitory effects of a dominant-interfering form of the Rho-GTPase Cdc42 in the chemoattractant-elicited signaling pathways leading to NADPH oxidase activation in differentiated HL-60 cells.* Blood, 2002. **100**(5): p. 1835-44.
44. Ruiz, S., E. Santos, and X.R. Bustelo, *RasGRF2, a guanosine nucleotide exchange factor for Ras GTPases, participates in T-cell signaling responses.* Mol Cell Biol, 2007. **27**(23): p. 8127-42.
45. Wei, W., et al., *Identification of a mammalian gene structurally and functionally related to the CDC25 gene of Saccharomyces cerevisiae.* Proc Natl Acad Sci U S A, 1992. **89**(15): p. 7100-4.
46. Cen, H., et al., *Regulated and constitutive activity by CDC25Mm (GRF), a Ras-specific exchange factor.* Mol Cell Biol, 1993. **13**(12): p. 7718-24.
47. Khosravi-Far, R. and C.J. Der, *The Ras signal transduction pathway.* Cancer Metastasis Rev, 1994. **13**(1): p. 67-89.
48. Quilliam, L.A., et al., *Membrane-targeting potentiates guanine nucleotide exchange factor CDC25 and SOS1 activation of Ras transforming activity.* Proc Natl Acad Sci U S A, 1994. **91**(18): p. 8512-6.
49. Tonini, R., et al., *Expression of Ras-GRF in the SK-N-BE neuroblastoma accelerates retinoic-acid-induced neuronal differentiation and increases the functional expression of the IRK1 potassium channel.* Eur J Neurosci, 1999. **11**(3): p. 959-66.
50. Baldassa, S., et al., *SCLIP, a microtubule-destabilizing factor, interacts with RasGRF1 and inhibits its ability to promote Rac activation and neurite outgrowth.* J Biol Chem, 2007. **282**(4): p. 2333-45.
51. Forlani, G., et al., *The guanine nucleotide exchange factor RasGRF1 directly binds microtubules via DHPH2-mediated interaction.* FEBS J, 2006. **273**(10): p. 2127-38.
52. Kesavapany, S., et al., *p35/cyclin-dependent kinase 5 phosphorylation of ras guanine nucleotide releasing factor 2 (RasGRF2) mediates Rac-dependent Extracellular Signal-regulated kinase 1/2 activity, altering RasGRF2 and microtubule-associated protein 1b distribution in neurons.* J Neurosci, 2004. **24**(18): p. 4421-31.
53. Sturani, E., et al., *The Ras Guanine nucleotide Exchange Factor CDC25Mm is present at the synaptic junction.* Exp Cell Res, 1997. **235**(1): p. 117-23.
54. Tonini, R., et al., *Involvement of CDC25Mm/Ras-GRF1-dependent signaling in the control of neuronal excitability.* Mol Cell Neurosci, 2001. **18**(6): p. 691-701.

55. Tian, X., et al., *Developmentally regulated role for Ras-GRFs in coupling NMDA glutamate receptors to Ras, Erk and CREB.* EMBO J, 2004. **23**(7): p. 1567-75.
56. Zhuravliova, E., et al., *Haloperidol induces neurotoxicity by the NMDA receptor downstream signaling pathway, alternative from glutamate excitotoxicity.* Neurochem Int, 2007. **50**(7-8): p. 976-82.
57. Li, D.W., et al., *Calcium-activated RAF/MEK/ERK signaling pathway mediates p53-dependent apoptosis and is abrogated by alpha B-crystallin through inhibition of RAS activation.* Mol Biol Cell, 2005. **16**(9): p. 4437-53.
58. Zhu, T.N., et al., *Filamin A-mediated down-regulation of the exchange factor Ras-GRF1 correlates with decreased matrix metalloproteinase-9 expression in human melanoma cells.* J Biol Chem, 2007. **282**(20): p. 14816-26.
59. Abreu, J.R., et al., *The Ras guanine nucleotide exchange factor RasGRF1 promotes matrix metalloproteinase-3 production in rheumatoid arthritis synovial tissue.* Arthritis Res Ther, 2009. **11**(4): p. R121.
60. Shin, D.M., et al., *Molecular characterization of isolated from murine adult tissues very small embryonic/epiblast like stem cells (VSELs).* Mol Cells. **29**(6): p. 533-8.
61. Hagihara, A., et al., *Identification of 27 5' CpG islands aberrantly methylated and 13 genes silenced in human pancreatic cancers.* Oncogene, 2004. **23**(53): p. 8705-10.
62. Jacinto, F.V., et al., *Discovery of epigenetically silenced genes by methylated DNA immunoprecipitation in colon cancer cells.* Cancer Res, 2007. **67**(24): p. 11481-6.
63. Chen, H., et al., *Aberrant methylation of RASGRF2 and RASSF1A in human non-small cell lung cancer.* Oncol Rep, 2006. **15**(5): p. 1281-5.
64. Qiu, C., et al., *Allelic imbalance and altered expression of genes in chromosome 2q11-2q16 from rat mammary gland carcinomas induced by 2-amino-1-methyl-6-phenylimidazo[4,5-b]pyridine.* Oncogene, 2003. **22**(8): p. 1253-60.
65. Ruiz, S., E. Santos, and X.R. Bustelo, *The use of knockout mice reveals a synergistic role of the Vav1 and Rasgrf2 gene deficiencies in lymphomagenesis and metastasis.* PLoS One, 2009. **4**(12): p. e8229.
66. Calvo, F., et al., *RasGRF suppresses Cdc42-mediated tumour cell movement, cytoskeletal dynamics and transformation.* Nat Cell Biol. **13**(7): p. 819-26.
67. Brambilla, R., et al., *A role for the Ras signalling pathway in synaptic transmission and long-term memory.* Nature, 1997. **390**(6657): p. 281-6.
68. Giese, K.P., et al., *Hippocampus-dependent learning and memory is impaired in mice lacking the Ras-guanine-nucleotide releasing factor 1 (Ras-GRF1).* Neuropharmacology, 2001. **41**(6): p. 791-800.
69. Fernandez-Medarde, A., et al., *RasGRF1 disruption causes retinal photoreception defects and associated transcriptomic alterations.* J Neurochem, 2009. **110**(2): p. 641-52.
70. Hysi, P.G., et al., *A genome-wide association study for myopia and refractive error identifies a susceptibility locus at 15q25.* Nat Genet, 2010. **42**(10): p. 902-5.
71. Rubino, T., et al., *Ras/ERK signalling in cannabinoid tolerance: from behaviour to cellular aspects.* J Neurochem, 2005. **93**(4): p. 984-91.
72. Rubino, T., et al., *Changes in the expression of G protein-coupled receptor kinases and beta-arrestins in mouse brain during cannabinoid tolerance: a role for RAS-ERK cascade.* Mol Neurobiol, 2006. **33**(3): p. 199-213.
73. Tonini, R., et al., *ERK-dependent modulation of cerebellar synaptic plasticity after chronic Delta9-tetrahydrocannabinol exposure.* J Neurosci, 2006. **26**(21): p. 5810-8.
74. Fasano, S., et al., *Ras-guanine nucleotide-releasing factor 1 (Ras-GRF1) controls activation of extracellular signal-regulated kinase (ERK) signaling in the striatum and long-term behavioral responses to cocaine.* Biol Psychiatry, 2009. **66**(8): p. 758-68.
75. Fernandez-Medarde, A., et al., *Targeted disruption of Ras-Grf2 shows its dispensability for mouse growth and development.* Mol Cell Biol, 2002. **22**(8): p. 2498-504.

76. Itier, J.M., et al., *Imprinted gene in postnatal growth role.* Nature, 1998. **393**(6681): p. 125-6.
77. Clapcott, S.J., et al., *Two ENU-induced mutations in Rasgrf1 and early mouse growth retardation.* Mamm Genome, 2003. **14**(8): p. 495-505.
78. Font de Mora, J., et al., *Ras-GRF1 signaling is required for normal beta-cell development and glucose homeostasis.* EMBO J, 2003. **22**(12): p. 3039-49.
79. Wang, Z., et al., *Pituitary tumor transforming gene-null male mice exhibit impaired pancreatic beta cell proliferation and diabetes.* Proc Natl Acad Sci U S A, 2003. **100**(6): p. 3428-32.
80. Pende, M., et al., *Hypoinsulinaemia, glucose intolerance and diminished beta-cell size in S6K1-deficient mice.* Nature, 2000. **408**(6815): p. 994-7.
81. Um, S.H., et al., *Absence of S6K1 protects against age- and diet-induced obesity while enhancing insulin sensitivity.* Nature, 2004. **431**(7005): p. 200-5.
82. Martin, J., et al., *Genetic rescue of Cdk4 null mice restores pancreatic beta-cell proliferation but not homeostatic cell number.* Oncogene, 2003. **22**(34): p. 5261-9.
83. Pei, L. and S. Melmed, *Isolation and characterization of a pituitary tumor-transforming gene (PTTG).* Mol Endocrinol, 1997. **11**(4): p. 433-41.
84. Zou, H., et al., *Identification of a vertebrate sister-chromatid separation inhibitor involved in transformation and tumorigenesis.* Science, 1999. **285**(5426): p. 418-22.
85. Dominguez, A., et al., *hpttg, a human homologue of rat pttg, is overexpressed in hematopoietic neoplasms. Evidence for a transcriptional activation function of hPTTG.* Oncogene, 1998. **17**(17): p. 2187-93.
86. Zhang, X., et al., *Structure, expression, and function of human pituitary tumor-transforming gene (PTTG).* Mol Endocrinol, 1999. **13**(1): p. 156-66.
87. Kakar, S.S. and L. Jennes, *Molecular cloning and characterization of the tumor transforming gene (TUTR1): a novel gene in human tumorigenesis.* Cytogenet Cell Genet, 1999. **84**(3-4): p. 211-6.
88. Boelaert, K., et al., *Pituitary tumor transforming gene and fibroblast growth factor-2 expression: potential prognostic indicators in differentiated thyroid cancer.* J Clin Endocrinol Metab, 2003. **88**(5): p. 2341-7.
89. Wang, Z. and S. Melmed, *Characterization of the murine pituitary tumor transforming gene (PTTG) and its promoter.* Endocrinology, 2000. **141**(2): p. 763-71.
90. Saez, C., et al., *hpttg is over-expressed in pituitary adenomas and other primary epithelial neoplasias.* Oncogene, 1999. **18**(39): p. 5473-6.
91. Hunter, J.A., et al., *The relationship between pituitary tumour transforming gene (PTTG) expression and in vitro hormone and vascular endothelial growth factor (VEGF) secretion from human pituitary adenomas.* Eur J Endocrinol, 2003. **148**(2): p. 203-11.
92. McCabe, C.J., et al., *Expression of pituitary tumour transforming gene (PTTG) and fibroblast growth factor-2 (FGF-2) in human pituitary adenomas: relationships to clinical tumour behaviour.* Clin Endocrinol (Oxf), 2003. **58**(2): p. 141-50.
93. Heaney, A.P., et al., *Transforming events in thyroid tumorigenesis and their association with follicular lesions.* J Clin Endocrinol Metab, 2001. **86**(10): p. 5025-32.
94. Shibata, Y., et al., *Expression of PTTG (pituitary tumor transforming gene) in esophageal cancer.* Jpn J Clin Oncol, 2002. **32**(7): p. 233-7.
95. Cho-Rok, J., et al., *Adenovirus-mediated transfer of siRNA against PTTG1 inhibits liver cancer cell growth in vitro and in vivo.* Hepatology, 2006. **43**(5): p. 1042-52.
96. Rehfeld, N., et al., *The influence of the pituitary tumor transforming gene-1 (PTTG-1) on survival of patients with small cell lung cancer and non-small cell lung cancer.* J Carcinog, 2006. **5**: p. 4.
97. Puri, R., et al., *Molecular cloning of pituitary tumor transforming gene 1 from ovarian tumors and its expression in tumors.* Cancer Lett, 2001. **163**(1): p. 131-9.

98. Tsai, S.J., et al., *Expression and functional analysis of pituitary tumor transforming gene-1 [corrected] in uterine leiomyomas.* J Clin Endocrinol Metab, 2005. **90**(6): p. 3715-23.
99. Tanaka, T., et al., *Cohesin ensures bipolar attachment of microtubules to sister centromeres and resists their precocious separation.* Nat Cell Biol, 2000. **2**(8): p. 492-9.
100. Uhlmann, F., F. Lottspeich, and K. Nasmyth, *Sister-chromatid separation at anaphase onset is promoted by cleavage of the cohesin subunit Scc1.* Nature, 1999. **400**(6739): p. 37-42.
101. Ciosk, R., et al., *An ESP1/PDS1 complex regulates loss of sister chromatid cohesion at the metaphase to anaphase transition in yeast.* Cell, 1998. **93**(6): p. 1067-76.
102. Hornig, N.C., et al., *The dual mechanism of separase regulation by securin.* Curr Biol, 2002. **12**(12): p. 973-82.
103. Waizenegger, I., et al., *Regulation of human separase by securin binding and autocleavage.* Curr Biol, 2002. **12**(16): p. 1368-78.
104. Stemmann, O., et al., *Dual inhibition of sister chromatid separation at metaphase.* Cell, 2001. **107**(6): p. 715-26.
105. Nasmyth, K., *How do so few control so many?* Cell, 2005. **120**(6): p. 739-46.
106. Wirth, K.G., et al., *Separase: a universal trigger for sister chromatid disjunction but not chromosome cycle progression.* J Cell Biol, 2006. **172**(6): p. 847-60.
107. Tong, Y., et al., *Pituitary tumor transforming gene interacts with Sp1 to modulate G1/S cell phase transition.* Oncogene, 2007. **26**(38): p. 5596-605.
108. Romero, F., et al., *Human securin, hPTTG, is associated with Ku heterodimer, the regulatory subunit of the DNA-dependent protein kinase.* Nucleic Acids Res, 2001. **29**(6): p. 1300-7.
109. Ptashne, M., *How eukaryotic transcriptional activators work.* Nature, 1988. **335**(6192): p. 683-9.
110. Wang, Z. and S. Melmed, *Pituitary tumor transforming gene (PTTG) transforming and transactivation activity.* J Biol Chem, 2000. **275**(11): p. 7459-61.
111. Pei, L., *Activation of mitogen-activated protein kinase cascade regulates pituitary tumor-transforming gene transactivation function.* J Biol Chem, 2000. **275**(40): p. 31191-8.
112. Horwitz, G.A., et al., *Human pituitary tumor-transforming gene (PTTG1) motif suppresses prolactin expression.* Mol Endocrinol, 2003. **17**(4): p. 600-9.
113. Pei, L., *Identification of c-myc as a down-stream target for pituitary tumor-transforming gene.* J Biol Chem, 2001. **276**(11): p. 8484-91.
114. Hamid, T., M.T. Malik, and S.S. Kakar, *Ectopic expression of PTTG1/securin promotes tumorigenesis in human embryonic kidney cells.* Mol Cancer, 2005. **4**(1): p. 3.
115. Mu, Y.M., et al., *Human pituitary tumor transforming gene (hPTTG) inhibits human lung cancer A549 cell growth through activation of p21(WAF1/CIP1).* Endocr J, 2003. **50**(6): p. 771-81.
116. Yu, R., et al., *Pituitary tumor transforming gene (PTTG) regulates placental JEG-3 cell division and survival: evidence from live cell imaging.* Mol Endocrinol, 2000. **14**(8): p. 1137-46.
117. Yu, R., et al., *Pituitary tumor transforming gene causes aneuploidy and p53-dependent and p53-independent apoptosis.* J Biol Chem, 2000. **275**(47): p. 36502-5.
118. Bernal, J.A., et al., *Human securin interacts with p53 and modulates p53-mediated transcriptional activity and apoptosis.* Nat Genet, 2002. **32**(2): p. 306-11.
119. Tfelt-Hansen, J., et al., *Expression of pituitary tumor transforming gene (PTTG) and its binding protein in human astrocytes and astrocytoma cells: function and regulation of PTTG in U87 astrocytoma cells.* Endocrinology, 2004. **145**(9): p. 4222-31.
120. Solbach, C., et al., *Pituitary tumor-transforming gene (PTTG): a novel target for anti-tumor therapy.* Anticancer Res, 2005. **25**(1A): p. 121-5.
121. Boelaert, K., et al., *A potential role for PTTG/securin in the developing human fetal brain.* FASEB J, 2003. **17**(12): p. 1631-9.

122. Boelaert, K., et al., *PTTG's C-terminal PXXP motifs modulate critical cellular processes in vitro.* J Mol Endocrinol, 2004. **33**(3): p. 663-77.
123. Romero, F., et al., *Securin is a target of the UV response pathway in mammalian cells.* Mol Cell Biol, 2004. **24**(7): p. 2720-33.
124. Yu, R., et al., *Overexpressed pituitary tumor-transforming gene causes aneuploidy in live human cells.* Endocrinology, 2003. **144**(11): p. 4991-8.
125. Jallepalli, P.V., et al., *Securin is required for chromosomal stability in human cells.* Cell, 2001. **105**(4): p. 445-57.
126. Pfleghaar, K., et al., *Securin is not required for chromosomal stability in human cells.* PLoS Biol, 2005. **3**(12): p. e416.
127. Hamid, T. and S.S. Kakar, *PTTG/securin activates expression of p53 and modulates its function.* Mol Cancer, 2004. **3**: p. 18.
128. Heaney, A.P., et al., *Expression of pituitary-tumour transforming gene in colorectal tumours.* Lancet, 2000. **355**(9205): p. 716-9.
129. Chien, W. and L. Pei, *A novel binding factor facilitates nuclear translocation and transcriptional activation function of the pituitary tumor-transforming gene product.* J Biol Chem, 2000. **275**(25): p. 19422-7.
130. Wang, Z., R. Yu, and S. Melmed, *Mice lacking pituitary tumor transforming gene show testicular and splenic hypoplasia, thymic hyperplasia, thrombocytopenia, aberrant cell cycle progression, and premature centromere division.* Mol Endocrinol, 2001. **15**(11): p. 1870-9.
131. Chesnokova, V., et al., *Pituitary hypoplasia in Pttg-/- mice is protective for Rb+/- pituitary tumorigenesis.* Mol Endocrinol, 2005. **19**(9): p. 2371-9.
132. Chesnokova, V., et al., *Diminished pancreatic beta-cell mass in securin-null mice is caused by beta-cell apoptosis and senescence.* Endocrinology, 2009. **150**(6): p. 2603-10.
133. Fraenkel, M., et al., *Sex-steroid milieu determines diabetes rescue in pttg-null mice.* J Endocrinol, 2006. **189**(3): p. 519-28.
134. Prieto, C. and J. De Las Rivas, *APID: Agile Protein Interaction DataAnalyzer.* Nucleic Acids Res, 2006. **34**(Web Server issue): p. W298-302.
135. Cline, M.S., et al., *Integration of biological networks and gene expression data using Cytoscape.* Nat Protoc, 2007. **2**(10): p. 2366-82.
136. Sawada, K., et al., *Hippocampal complexin proteins and cognitive dysfunction in schizophrenia.* Arch Gen Psychiatry, 2005. **62**(3): p. 263-72.
137. Bach, M.E., et al., *Impairment of spatial but not contextual memory in CaMKII mutant mice with a selective loss of hippocampal LTP in the range of the theta frequency.* Cell, 1995. **81**(6): p. 905-15.
138. Heimann, M., et al., *Sublingual and submandibular blood collection in mice: a comparison of effects on body weight, food consumption and tissue damage.* Lab Anim, 2010. **44**(4): p. 352-8.
139. Clem, A.L., T. Hamid, and S.S. Kakar, *Characterization of the role of Sp1 and NF-Y in differential regulation of PTTG/securin expression in tumor cells.* Gene, 2003. **322**: p. 113-21.
140. Whitmarsh, A.J., et al., *Integration of MAP kinase signal transduction pathways at the serum response element.* Science, 1995. **269**(5222): p. 403-7.
141. Marais, R., J. Wynne, and R. Treisman, *The SRF accessory protein Elk-1 contains a growth factor-regulated transcriptional activation domain.* Cell, 1993. **73**(2): p. 381-93.
142. Datta, R., et al., *Reactive oxygen intermediates target CC(A/T)6GG sequences to mediate activation of the early growth response 1 transcription factor gene by ionizing radiation.* Proc Natl Acad Sci U S A, 1993. **90**(6): p. 2419-22.
143. Lim, C.P., N. Jain, and X. Cao, *Stress-induced immediate-early gene, egr-1, involves activation of p38/JNK1.* Oncogene, 1998. **16**(22): p. 2915-26.

144. Sartipy, P. and D.J. Loskutoff, *Expression profiling identifies genes that continue to respond to insulin in adipocytes made insulin-resistant by treatment with tumor necrosis factor-alpha.* J Biol Chem, 2003. **278**(52): p. 52298-306.
145. Tarcic, G., et al., *EGR1 and the ERK-ERF axis drive mammary cell migration in response to EGF.* FASEB J, 2011. **26**(4): p. 1582-92.
146. Kuroda, K.O., et al., *ERK-FosB signaling in dorsal MPOA neurons plays a major role in the initiation of parental behavior in mice.* Mol Cell Neurosci, 2007. **36**(2): p. 121-31.
147. Lazo, P.S., et al., *Structure and mapping of the fosB gene. FosB downregulates the activity of the fosB promoter.* Nucleic Acids Res, 1992. **20**(2): p. 343-50.
148. Wang, W., et al., *Identification of small-molecule inducers of pancreatic beta-cell expansion.* Proc Natl Acad Sci U S A, 2009. **106**(5): p. 1427-32.
149. Gao, N., et al., *Dynamic regulation of Pdx1 enhancers by Foxa1 and Foxa2 is essential for pancreas development.* Genes Dev, 2008. **22**(24): p. 3435-48.
150. Gao, N., et al., *Foxa1 and Foxa2 maintain the metabolic and secretory features of the mature beta-cell.* Mol Endocrinol, 2010. **24**(8): p. 1594-604.
151. Simmons, D.M., et al., *Pituitary cell phenotypes involve cell-specific Pit-1 mRNA translation and synergistic interactions with other classes of transcription factors.* Genes Dev, 1990. **4**(5): p. 695-711.
152. Dolle, P., et al., *Expression of GHF-1 protein in mouse pituitaries correlates both temporally and spatially with the onset of growth hormone gene activity.* Cell, 1990. **60**(5): p. 809-20.
153. Lefevre, C., et al., *Tissue-specific expression of the human growth hormone gene is conferred in part by the binding of a specific trans-acting factor.* EMBO J, 1987. **6**(4): p. 971-81.
154. Gil-Puig, C., et al., *Pit-1 is expressed in normal and tumorous human breast and regulates GH secretion and cell proliferation.* Eur J Endocrinol, 2005. **153**(2): p. 335-44.
155. Kim, D., et al., *Pituitary tumour transforming gene (PTTG) induces genetic instability in thyroid cells.* Oncogene, 2005. **24**(30): p. 4861-6.
156. Abbud, R.A., et al., *Early multipotential pituitary focal hyperplasia in the alpha-subunit of glycoprotein hormone-driven pituitary tumor-transforming gene transgenic mice.* Mol Endocrinol, 2005. **19**(5): p. 1383-91.
157. Greene, L.A. and A.S. Tischler, *Establishment of a noradrenergic clonal line of rat adrenal pheochromocytoma cells which respond to nerve growth factor.* Proc Natl Acad Sci U S A, 1976. **73**(7): p. 2424-8.
158. Fernandez-Medarde, A., et al., *Laser microdissection and microarray analysis of the hippocampus of Ras-GRF1 knockout mice reveals gene expression changes affecting signal transduction pathways related to memory and learning.* Neuroscience, 2007. **146**(1): p. 272-85.
159. Liang, M., et al., *Role of the pituitary tumor transforming gene 1 in the progression of hepatocellular carcinoma.* Cancer Biol Ther, 2010. **11**(3): p. 337-45.
160. Liu, C.L., et al., *L2dtl is essential for cell survival and nuclear division in early mouse embryonic development.* J Biol Chem, 2007. **282**(2): p. 1109-18.
161. Yuen, K., *Chromosome Instability (CIN), Aneuploidy and Cancer.* eLS, 2010.
162. Musacchio, A. and E.D. Salmon, *The spindle-assembly checkpoint in space and time.* Nat Rev Mol Cell Biol, 2007. **8**(5): p. 379-93.
163. Peters, J.M., *The anaphase promoting complex/cyclosome: a machine designed to destroy.* Nat Rev Mol Cell Biol, 2006. **7**(9): p. 644-56.
164. Sullivan, M. and D.O. Morgan, *Finishing mitosis, one step at a time.* Nat Rev Mol Cell Biol, 2007. **8**(11): p. 894-903.
165. Malumbres, M. and M. Barbacid, *Cell cycle, CDKs and cancer: a changing paradigm.* Nat Rev Cancer, 2009. **9**(3): p. 153-66.

166. Perez de Castro, I., G. de Carcer, and M. Malumbres, *A census of mitotic cancer genes: new insights into tumor cell biology and cancer therapy.* Carcinogenesis, 2007. **28**(5): p. 899-912.
167. Carter, S.L., et al., *A signature of chromosomal instability inferred from gene expression profiles predicts clinical outcome in multiple human cancers.* Nat Genet, 2006. **38**(9): p. 1043-8.
168. Fukasawa, K., *Oncogenes and tumour suppressors take on centrosomes.* Nat Rev Cancer, 2007. **7**(12): p. 911-24.
169. Yu, R., et al., *Murine pituitary tumor-transforming gene functions as a securin protein in insulin-secreting cells.* J Endocrinol, 2006. **191**(1): p. 45-53.
170. Marshall, C.J., *Specificity of receptor tyrosine kinase signaling: transient versus sustained extracellular signal-regulated kinase activation.* Cell, 1995. **80**(2): p. 179-85.
171. York, R.D., et al., *Rap1 mediates sustained MAP kinase activation induced by nerve growth factor.* Nature, 1998. **392**(6676): p. 622-6.
172. Meakin, S.O., et al., *The signaling adapter FRS-2 competes with Shc for binding to the nerve growth factor receptor TrkA. A model for discriminating proliferation and differentiation.* J Biol Chem, 1999. **274**(14): p. 9861-70.
173. Pozzan, T., et al., *Ca2+-dependent and -independent release of neurotransmitters from PC12 cells: a role for protein kinase C activation?* J Cell Biol, 1984. **99**(2): p. 628-38.
174. Carpenter, G. and S. Cohen, *Epidermal growth factor.* J Biol Chem, 1990. **265**(14): p. 7709-12.
175. Mendoza, M.C., E.E. Er, and J. Blenis, *The Ras-ERK and PI3K-mTOR pathways: cross-talk and compensation.* Trends Biochem Sci, 2011. **36**(6): p. 320-8.
176. Holmes, A., et al., *Behavioral profiles of inbred strains on novel olfactory, spatial and emotional tests for reference memory in mice.* Genes Brain Behav, 2002. **1**(1): p. 55-69.
177. Barr, A.M., et al., *Altered performance of reelin-receptor ApoER2 deficient mice on spatial tasks using the Barnes maze.* Behav Neurosci, 2007. **121**(5): p. 1101-5.
178. d'Isa, R., et al., *Mice Lacking Ras-GRF1 Show Contextual Fear Conditioning but not Spatial Memory Impairments: Convergent Evidence from Two Independently Generated Mouse Mutant Lines.* Front Behav Neurosci, 2011. **5**: p. 78.
179. Christie, J.M., R.J. Wenthold, and D.T. Monaghan, *Insulin causes a transient tyrosine phosphorylation of NR2A and NR2B NMDA receptor subunits in rat hippocampus.* J Neurochem, 1999. **72**(4): p. 1523-8.
180. Muller, A.P., et al., *Exercise increases insulin signaling in the hippocampus: physiological effects and pharmacological impact of intracerebroventricular insulin administration in mice.* Hippocampus, 2010. **21**(10): p. 1082-92.
181. Thompson, A.D., 3rd and S.S. Kakar, *Insulin and IGF-1 regulate the expression of the pituitary tumor transforming gene (PTTG) in breast tumor cells.* FEBS Lett, 2005. **579**(14): p. 3195-200.
182. Chamaon, K., et al., *Regulation of the pituitary tumor transforming gene by insulin-like-growth factor-I and insulin differs between malignant and non-neoplastic astrocytes.* Biochem Biophys Res Commun, 2005. **331**(1): p. 86-92.
183. Mauras, N., et al., *Sex steroids, growth hormone, insulin-like growth factor-1: neuroendocrine and metabolic regulation in puberty.* Horm Res, 1996. **45**(1-2): p. 74-80.
184. George, M., et al., *Beta cell expression of IGF-I leads to recovery from type 1 diabetes.* J Clin Invest, 2002. **109**(9): p. 1153-63.

NAME (UNIPROT)	DESCRIPTION
HDAC7_HUMAN	Histone deacetylase 7
HD_HUMAN	Huntingtin
PIAS1_HUMAN	E3 SUMO-protein ligase PIAS1
G3P_HUMAN	Glyceraldehyde-3-phosphate dehydrogenase
TF2AA_HUMAN	Transcription initiation factor IIA subunit 1
HDAC1-HUMAN	Histone deacetylase 1
CUL1_HUMAN	Cullin-1
MEF2D_HUMAN	Myocyte-specific enhancer factor 2D
LT_SV40	Large T antigen
SMCA4_HUMAN	Probable global transcription activator SNF2L4
TF3B_HUMAN	Transcription factor IIIB 90 kDa subunit
WWTR1_HUMAN	WW domain-containing transcription regulator protein 1
HNF4A-HUMAN	Hepatocyte nuclear factor 4-alpha
CCND1_HUMAN	G1/S-specific cyclin-D1
PML_HUMAN	Probable transcription factor PML
ARI3A_HUMAN	AT-rich interactive domain-containing protein 3A
CCNA2_HUMAN	Cyclin-A2
TAF1B-HUMAN	TATA box-binding protein-associated factor RNA polymerase I subunit B
CDK7_HUMAN	Cell division protein kinase 7
NUCL_HUMAN	Nucleolin
TF2H1_HUMAN	General transcription factor IIH subunit 1
ANDR-HUMAN	Androgen receptor
HMGB2-HUMAN	High mobility group protein B2
CEBPB_HUMAN	CCAAT/enhancer-binding protein beta
FOXO1-HUMAN	Forkhead box protein O1
P73_HUMAN	Tumor protein p73
PCAF_HUMAN	Histone acetyltransferase PCAF
CABL1-MOUSE	CDK5 and ABL1 enzyme substrate 1
HSF1_HUMAN	Heat shock factor protein 1
PHB_HUMAN	Prohibitin
PARP1-HUMAN	Poly "ADP-ribose" polymerase 1
2AAA_HUMAN	Serine/threonine-protein phosphatase 2A 65 kDa regulatory subunit A alpha isoform
SUMO3_HUMAN	Small ubiquitin-related modifier 3
PCTK2_HUMAN	Serine/threonine-protein kinase PCTAIRE-2
VE6_HPV18	Protein E6
ATF3_HUMAN	Cyclic AMP-dependent transcription factor ATF-3
ATR_HUMAN	Serine/threonine-protein kinase ATR
HIPK1_HUMAN	Homeodomain-interacting protein kinase 1
JUN_HUMAN	Transcription factor AP-1
CREM_HUMAN	cAMP-responsive element modulator
KU70_HUMAN	ATP-dependent DNA helicase 2 subunit 1

CDC2_HUMAN	Cell division control protein 2 homolog
TAF9_HUMAN	Transcription initiation factor TFIID subunit 9
SET_HUMAN	Protein SET
FOS_HUMAN	Proto-oncogene protein c-fos
TFDP1-HUMAN	Transcription factor Dp-1
RUVB2_HUMAN	RuvB-like 2
NF1_HUMAN	Neurofibromin
GCR-HUMAN	Glucocorticoid receptor
TFDP2_HUMAN	Transcription factor Dp-2
TIP60_HUMAN	Histone acetyltransferase HTATIP
TAF1C-HUMAN	TATA box-binding protein-associated factor RNA polymerase I subunit C
MAT1_HUMAN	CDK-activating kinase assembly factor MAT1
SYEP_HUMAN	Bifunctional aminoacyl-tRNA synthetase
CSK21_HUMAN	Casein kinase II subunit alpha
SMRC1-HUMAN	SWI/SNF complex subunit SMARCC1
DAXX_HUMAN	Death domain-associated protein 6
TAZ_HUMAN	Tafazzin
ATF1_HUMAN	Cyclic AMP-dependent transcription factor ATF-1
IASPP_HUMAN	RelA-associated inhibitor
NFKB1-HUMAN	Nuclear factor NF-kappa-B p105 subunit
MDM4_HUMAN	Protein Mdm4
FHL2_HUMAN	Four and a half LIM domains protein 2
MK01-HUMAN	Mitogen-activated protein kinase 1
UBC9-HUMAN	SUMO-conjugating enzyme UBC9
NMDZ1_HUMAN	Glutamate "NMDA" receptor subunit zeta-1
RB_HUMAN	Retinoblastoma-associated protein
GRB2_HUMAN	Growth factor receptor-bound protein 2
MIP_HUMAN	Lens fiber major intrinsic protein
NECD-HUMAN	Necdin
SP1-HUMAN	Transcription factor Sp1
CABL1-HUMAN	CDK5 and ABL1 enzyme substrate 1
HSP7C_HUMAN	Heat shock cognate 71 kDa protein
ABL1-HUMAN	Proto-oncogene tyrosine-protein kinase ABL1
RUVB1_HUMAN	RuvB-like 1
NFYB_HUMAN	Nuclear transcription factor Y subunit beta
NCOA1_HUMAN	Nuclear receptor coactivator 1
SMAD4_HUMAN	Mothers against decapentaplegic homolog 4
CASP8_HUMAN	Caspase-8
TF65_HUMAN	Transcription factor p65
SMAD2_HUMAN	Mothers against decapentaplegic homolog 2
CASP3_HUMAN	Caspase-3
SYUA_HUMAN	Alpha-synuclein
P53_HUMAN	Cellular tumor antigen p53
SMAD3_HUMAN	Mothers against decapentaplegic homolog 3

MED1_HUMAN	Mediator of RNA polymerase II transcription subunit 1
TP53B_HUMAN	Tumor suppressor p53-binding protein 1
TBP-HUMAN	TATA-box-binding protein
YAP1_HUMAN	65 kDa Yes-associated protein
HIPK2_HUMAN	Homeodomain-interacting protein kinase 2
SNF5_HUMAN	SWI/SNF-related matrix-associated actin-dependent regulator of chromatin subfamily B member 1
MSX1_HUMAN	Homeobox protein MSX-1
MK11-HUMAN	Mitogen-activated protein kinase 11
SRC_HUMAN	Proto-oncogene tyrosine-protein kinase Src
CHD3_HUMAN	Chromodomain-helicase-DNA-binding protein 3
MYC_HUMAN	Myc proto-oncogene protein
DHX9_HUMAN	ATP-dependent RNA helicase A
E2F1-HUMAN	Transcription factor E2F1
IFI5B_MOUSE	Interferon-activable protein 205-B
EGR1_HUMAN	Early growth response protein 1
FYN_HUMAN	Proto-oncogene tyrosine-protein kinase Fyn
PABP4_HUMAN	Polyadenylate-binding protein 4
BRCA1_HUMAN	Breast cancer type 1 susceptibility protein
MK08-HUMAN	Mitogen-activated protein kinase 8
AKT1_HUMAN	RAC-alpha serine/threonine-protein kinase
HDAC4_HUMAN	Histone deacetylase 4
NCK1_HUMAN	Cytoplasmic protein NCK1
MTA2_HUMAN	Metastasis-associated protein MTA2
TAF1A-HUMAN	TATA box-binding protein-associated factor RNA polymerase I subunit A
NFYA-HUMAN	Nuclear transcription factor Y subunit alpha
IKZF3-HUMAN	Zinc finger protein Aiolos
NCOA2_HUMAN	Nuclear receptor coactivator 2
CDK2_HUMAN	Cell division protein kinase 2
SP3_HUMAN	Transcription factor Sp3
CDN1A-HUMAN	Cyclin-dependent kinase inhibitor 1
KPCD_HUMAN	Protein kinase C delta type
VRK1_HUMAN	Serine/threonine-protein kinase VRK1
TAF1-HUMAN	Transcription initiation factor TFIID subunit 1
TAF6-HUMAN	Transcription initiation factor TFIID subunit 6
H2B2E_HUMAN	Histone H2B type 2-E
STAT3_HUMAN	Signal transducer and activator of transcription 3
PRKDC_HUMAN	DNA-dependent protein kinase catalytic subunit
PIAS2_HUMAN	E3 SUMO-protein ligase PIAS2
MK09_HUMAN	Mitogen-activated protein kinase 9
T2AG_HUMAN	Transcription initiation factor IIA subunit 2
PTEN-HUMAN	Phosphatidylinositol-3,4,5-trisphosphate 3-phosphatase and dual-specificity protein phosphatase
TYY1_HUMAN	Transcriptional repressor protein YY1
THA_HUMAN	Thyroid hormone receptor alpha

MP2K1_HUMAN	Dual specificity mitogen-activated protein kinase kinase 1
RBL1_HUMAN	Retinoblastoma-like protein 1
SAP18_HUMAN	Histone deacetylase complex subunit SAP18
HIF1A_HUMAN	Hypoxia-inducible factor 1 alpha
KLF4_HUMAN	Krueppel-like factor 4
CSN2_HUMAN	COP9 signalosome complex subunit 2
MCM2_HUMAN	DNA replication licensing factor MCM2
EP300_HUMAN	Histone acetyltransferase p300
MAPK5_HUMAN	MAP kinase-activated protein kinase 5
SUMO1-HUMAN	Small ubiquitin-related modifier 1
GSK3B_HUMAN	Glycogen synthase kinase-3 beta
HMGB1_HUMAN	High mobility group protein B1
KLF6_HUMAN	Krueppel-like factor 6
CDK5-HUMAN	Cell division protein kinase 5
MK03-HUMAN	Mitogen-activated protein kinase 3
CD2A2_HUMAN	Cyclin-dependent kinase inhibitor 2A, isoform 4
GCR-MOUSE	Glucocorticoid receptor
CHK2_HUMAN	Serine/threonine-protein kinase Chk2
CBP_HUMAN	CREB-binding protein
NCOR2_HUMAN	Nuclear receptor corepressor 2
ESR1_HUMAN	Estrogen receptor
HNRPK_HUMAN	Heterogeneous nuclear ribonucleoprotein K
ESR2_HUMAN	Estrogen receptor beta
CSN7A_HUMAN	COP9 signalosome complex subunit 7a
SIN3A-HUMAN	Paired amphipathic helix protein Sin3a
MDM2-HUMAN	E3 ubiquitin-protein ligase Mdm2
UBIQ_HUMAN	Ubiquitin
NCOA3_HUMAN	Nuclear receptor coactivator 3
VE2-HPV16	Regulatory protein E2
MK07_HUMAN	Mitogen-activated protein kinase 7
BARD1_HUMAN	BRCA1-associated RING domain protein 1

Pttg1 mice

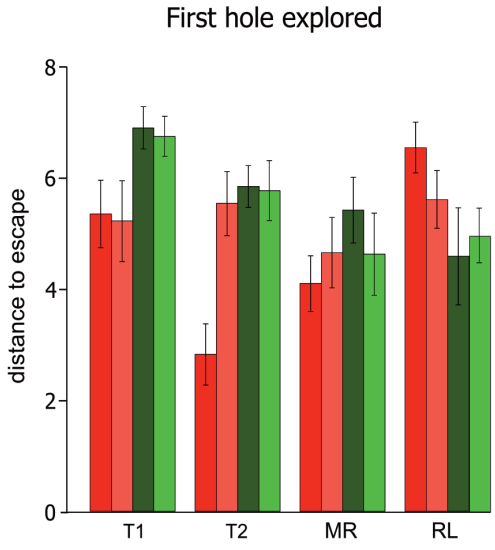
First hole explored
distance to escape
0
2
4
6
8
T1
T2
MR
RL

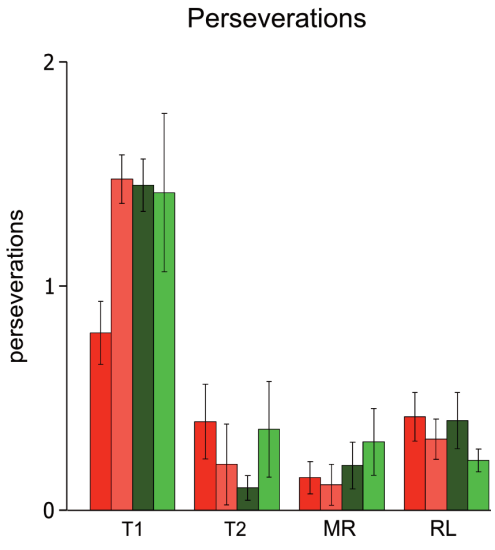
Perseverations
perseverations
0
1
2
T1
T2
MR
RL

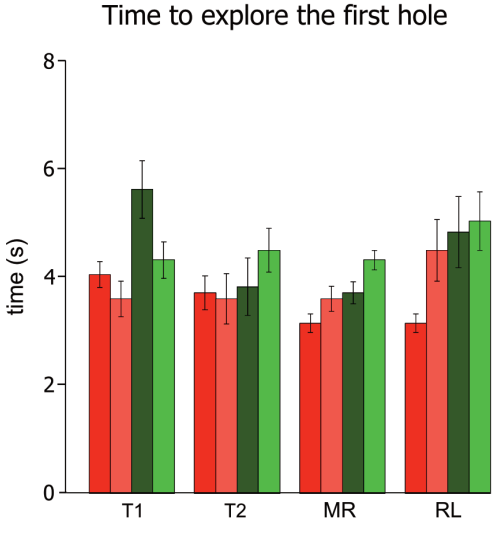
Time to explore the first hole
time (s)
0
2
4
6
8
T1
T2
MR
RL

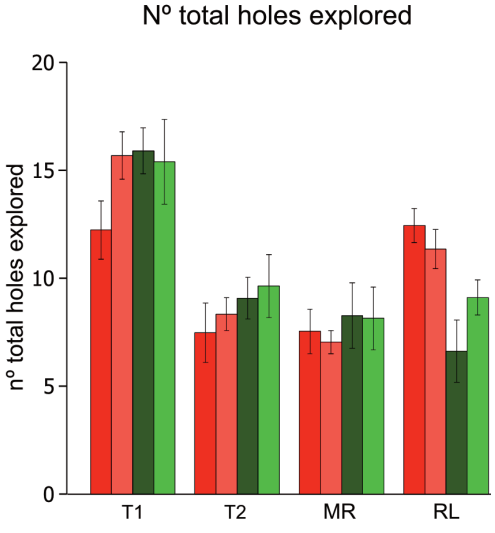
Nº total holes explored
nº total holes explored
0
5
10
15
20
T1
T2
MR
RL

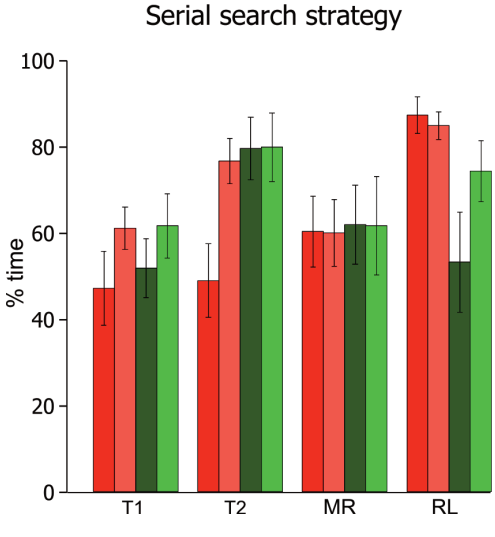
Serial search strategy
% time
0
20
40
60
80
100
T1
T2
MR
RL

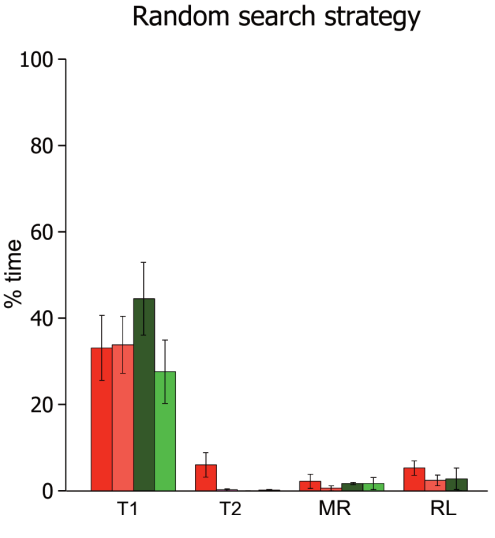
Random search strategy
% time
0
20
40
60
80
100
T1
T2
MR
RL

RasGrf1 mice

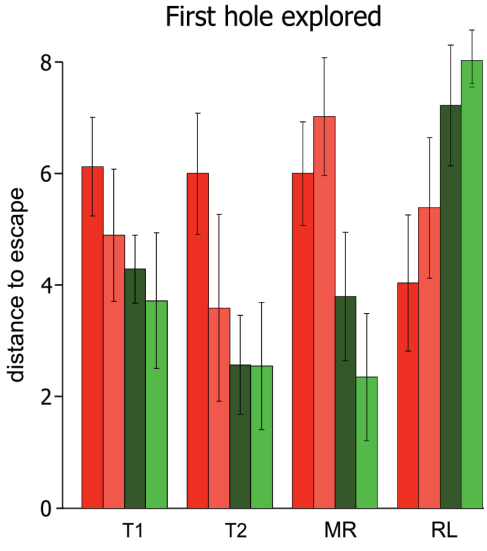

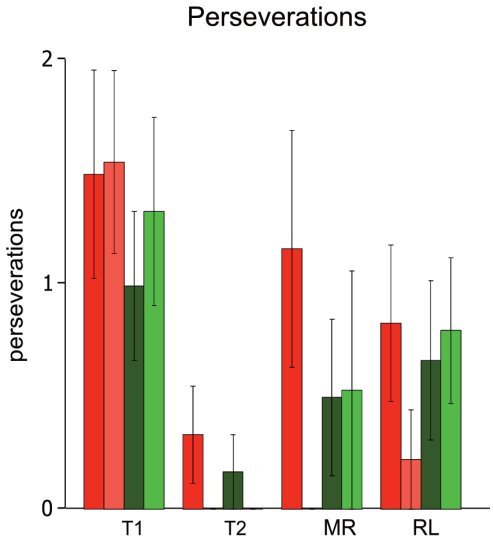

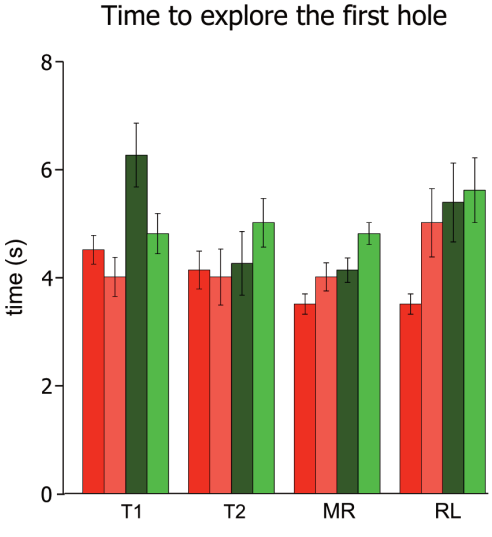

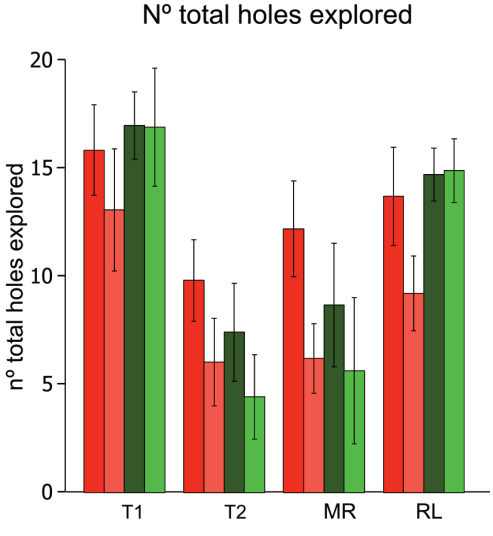

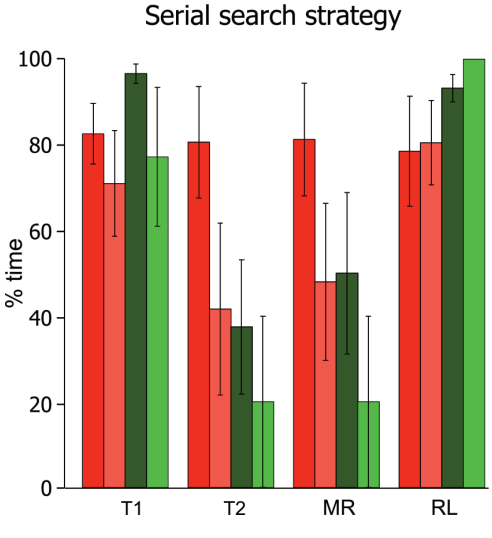

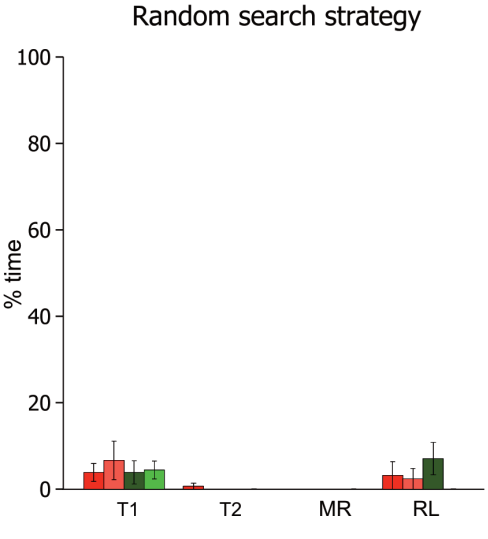

RasGrf1-Pttg1 mice